

SUPPORTING INFORMATION

Luminescent cyclometalated alkynylplatinum(II) complexes with 1,3-di(pyrimidin-2-yl)benzene ligands: synthesis, electrochemistry, photophysics and computational studies

Mariia Hruzd,^a Nicolas le Poul,^b Marie Cordier,^a Samia Kahlal,^a Jean-Yves Saillard,^a Sylvain

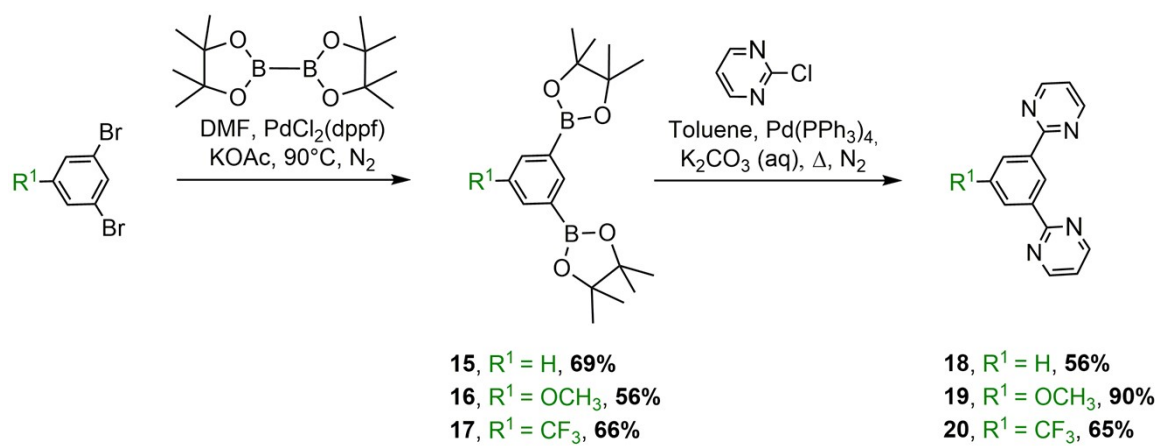
Achelle,^{a*} Sébastien Gauthier,^{a*} and Françoise Robin-le Guen^{a*}

^a Univ. Rennes, CNRS, ISCR (Institut des Sciences Chimiques de Rennes) - UMR 6226, F-35000 Rennes, France. E-mails: sylvain.achelle@univ-rennes1.fr, sebastien.gauthier@univ-rennes1.fr francoise.le-guen@univ-rennes1.fr

^b Laboratoire de Chimie, Électrochimie Moléculaires et Chimie Analytique, UMR CNRS 6521, Université de Bretagne Occidentale, UFR Sciences et Techniques, 6 avenue Victor Le Gorgeu – CS 93837, F-29238 Brest Cedex 3, France.

Table of content

| | |
|--|----|
| Synthesis of the N [^] C [^] N ligands 18-20 | 2 |
| NMR Spectra of ligand 20 | 3 |
| NMR Spectra of complexes 4-14 | 4 |
| Mass spectra ESI-MS of complexes 3-14 and ligand 20 | 15 |
| Crystallographic Data for 7 and 8 | 17 |
| Additional Cyclic Voltammetry | 19 |
| Additional Photophysical Data | 20 |
| Additional Theoretical Results | 26 |
| References | 40 |



Scheme S1 Synthesis of the N^CN ligands **18-20**.

NMR Spectra of ligand **20**

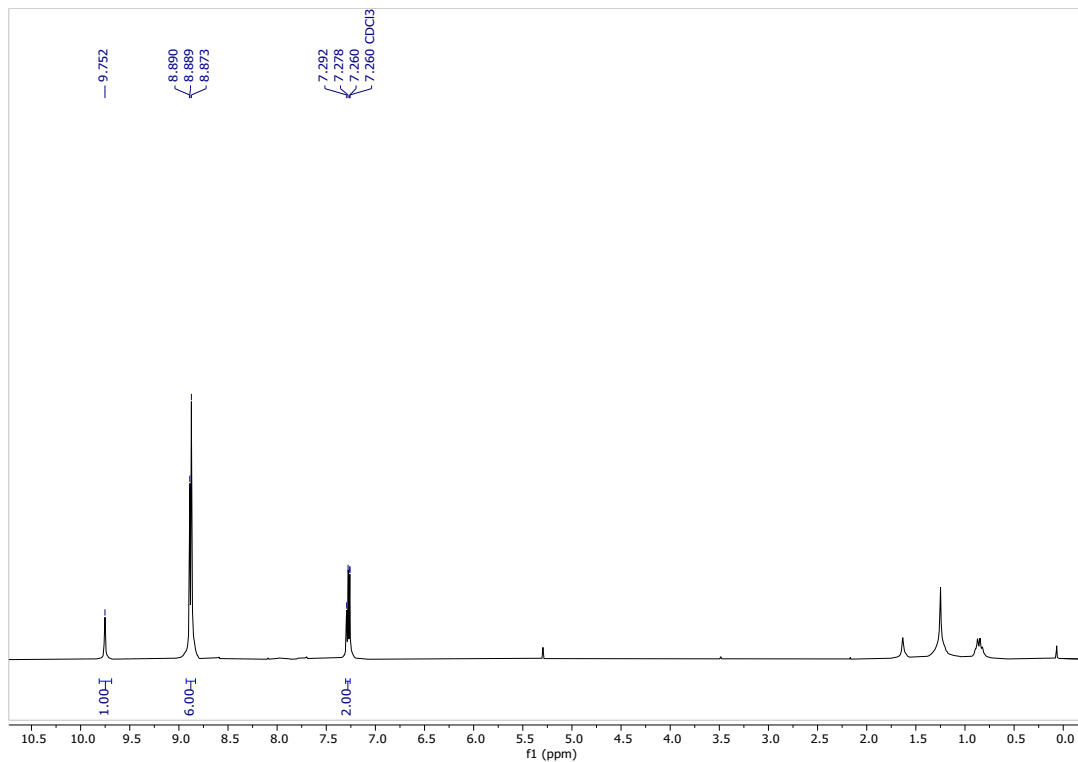
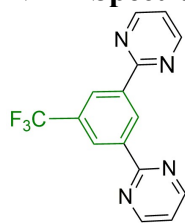


Fig. S1 ^1H NMR spectrum (300 MHz, CDCl_3) of **20**.

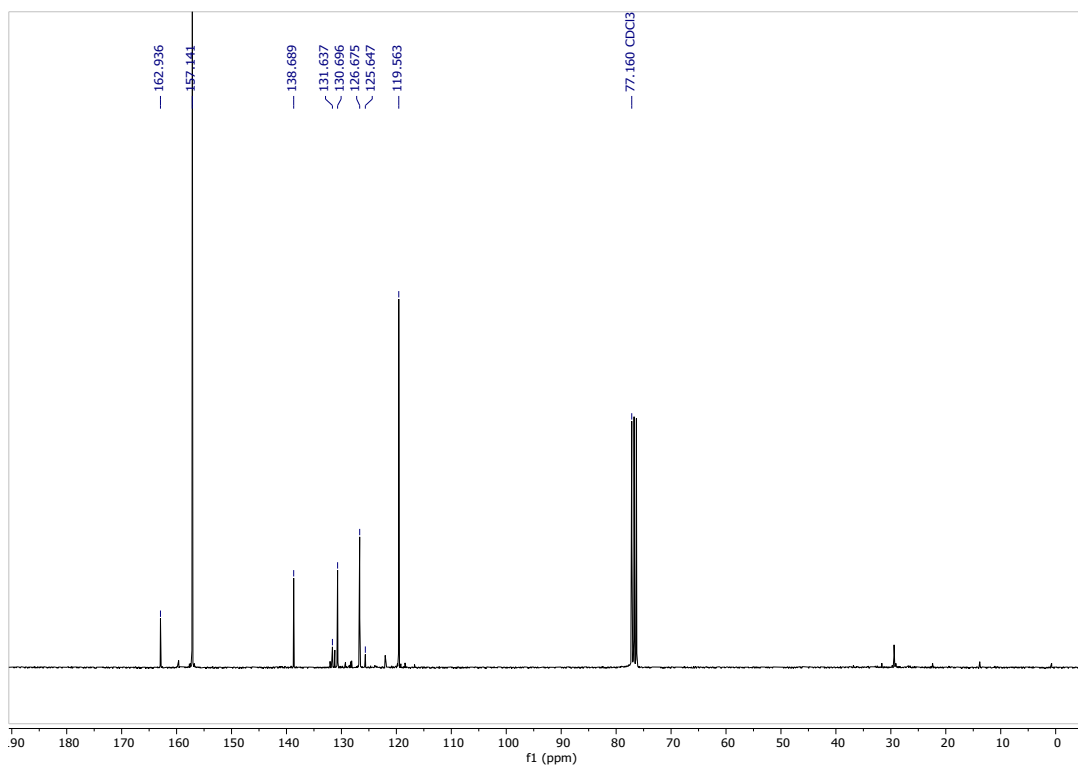


Fig. S2 ^{13}C NMR spectrum (75 MHz, CDCl_3) of **20**.

Complex 4

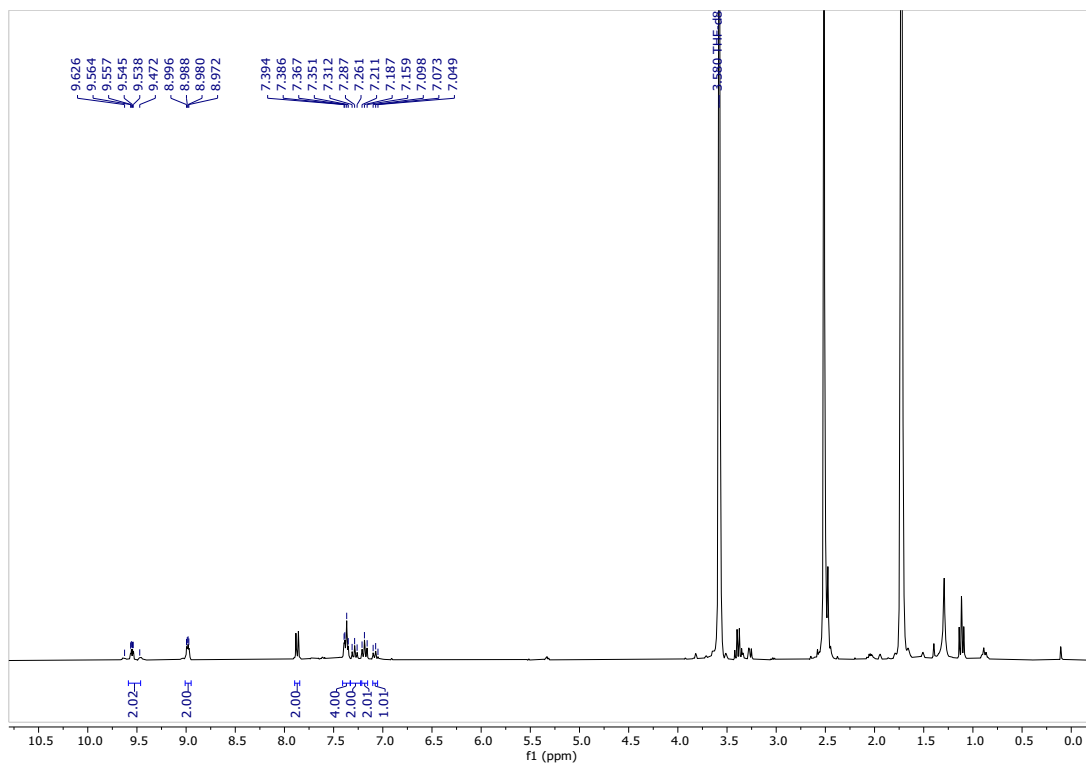
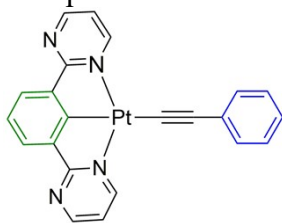


Fig. S3 ^1H NMR spectrum (300 MHz, THF-d8) of 4.

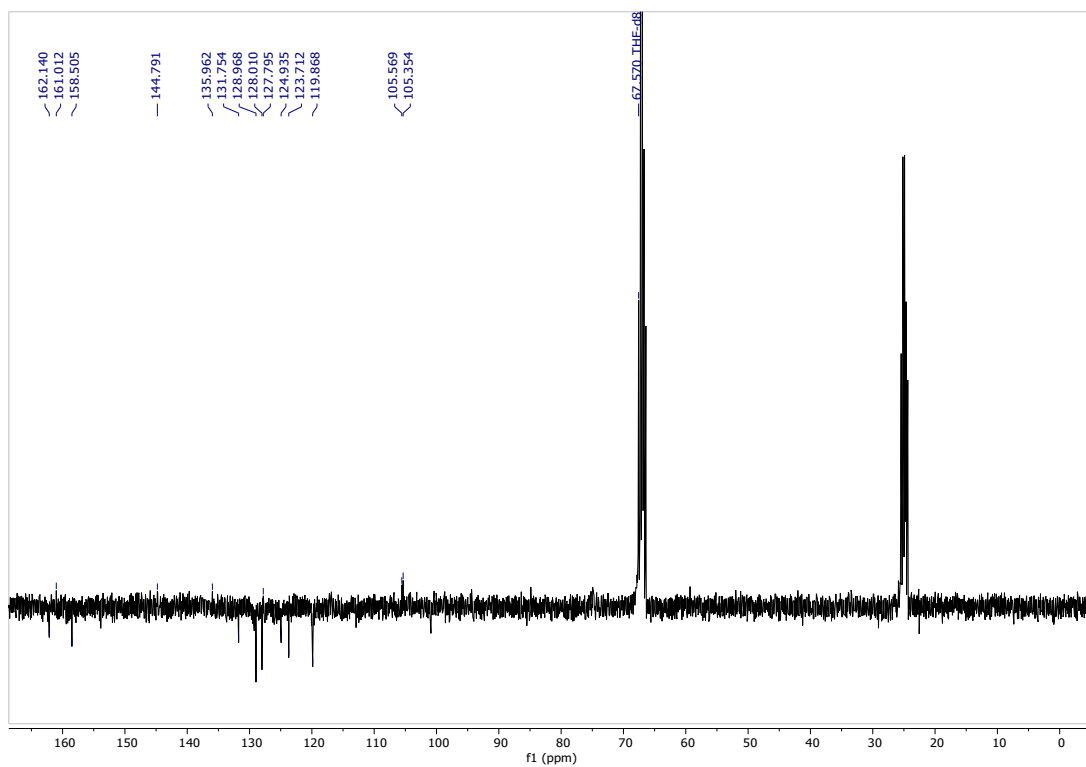


Fig. S4 ^{13}C NMR spectrum (JMOD, 75 MHz, THF-d8) of 4.

Complex 5

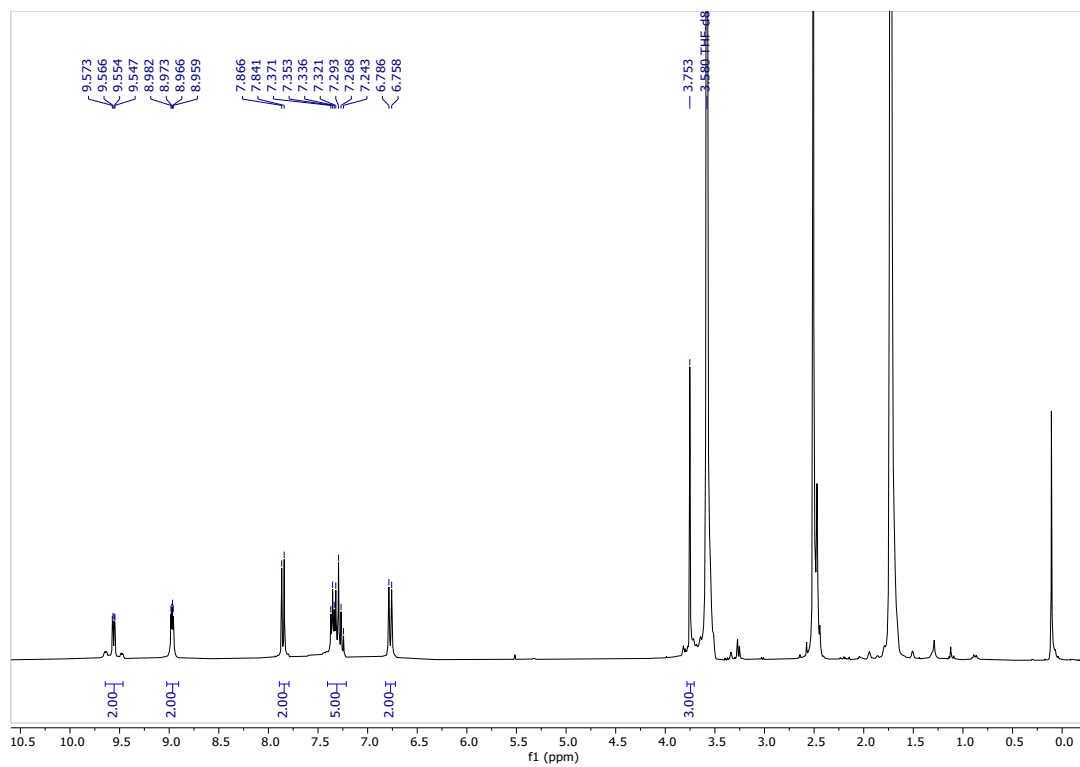
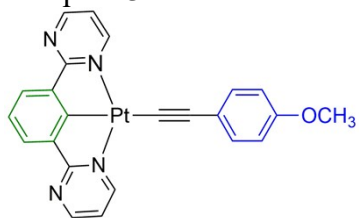


Fig. S5 ^1H NMR spectrum (300 MHz, THF-d8) of 5.

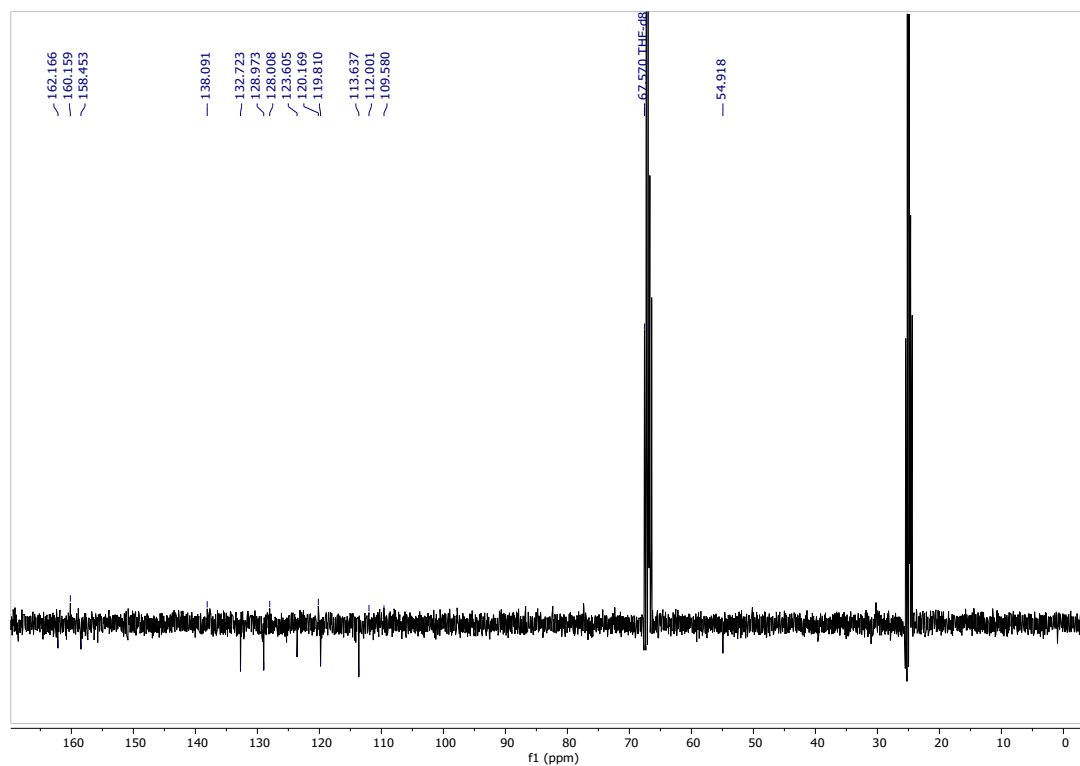


Fig. S6 ^{13}C NMR spectrum (JMOD, 75 MHz, THF-d8) of 5.

Complex 6

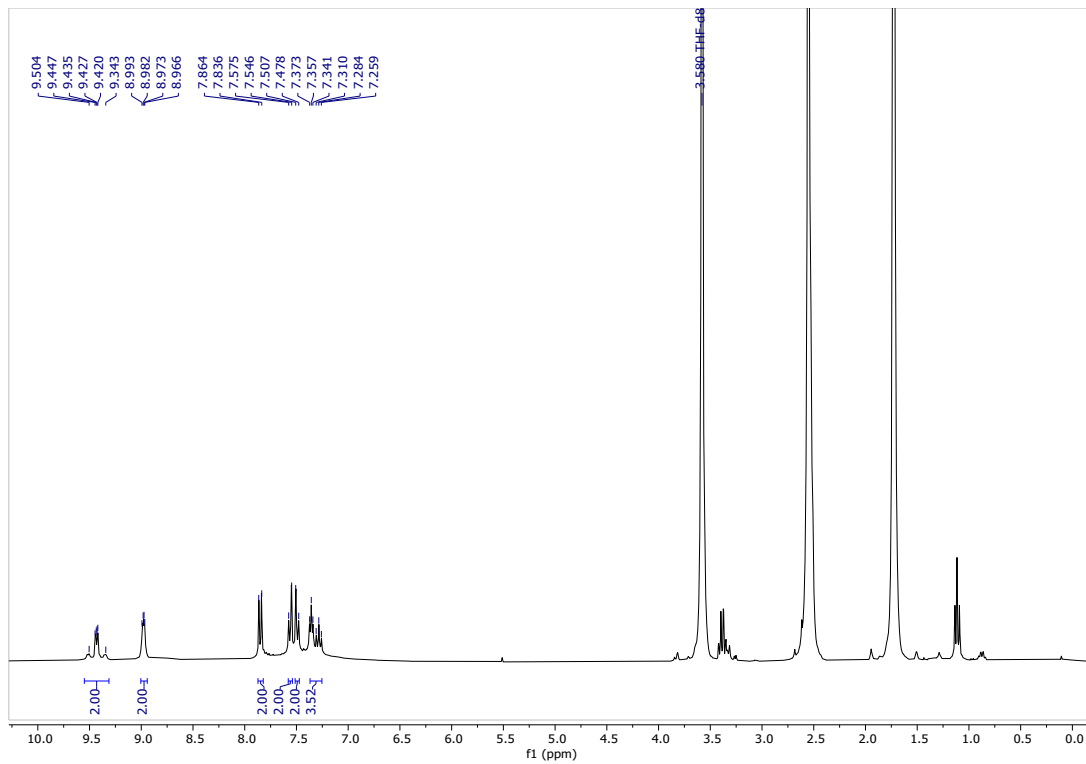
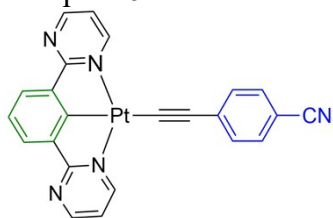


Fig. S7 ¹H NMR spectrum (300 MHz, THF-d₈) of 6.

Complex 7

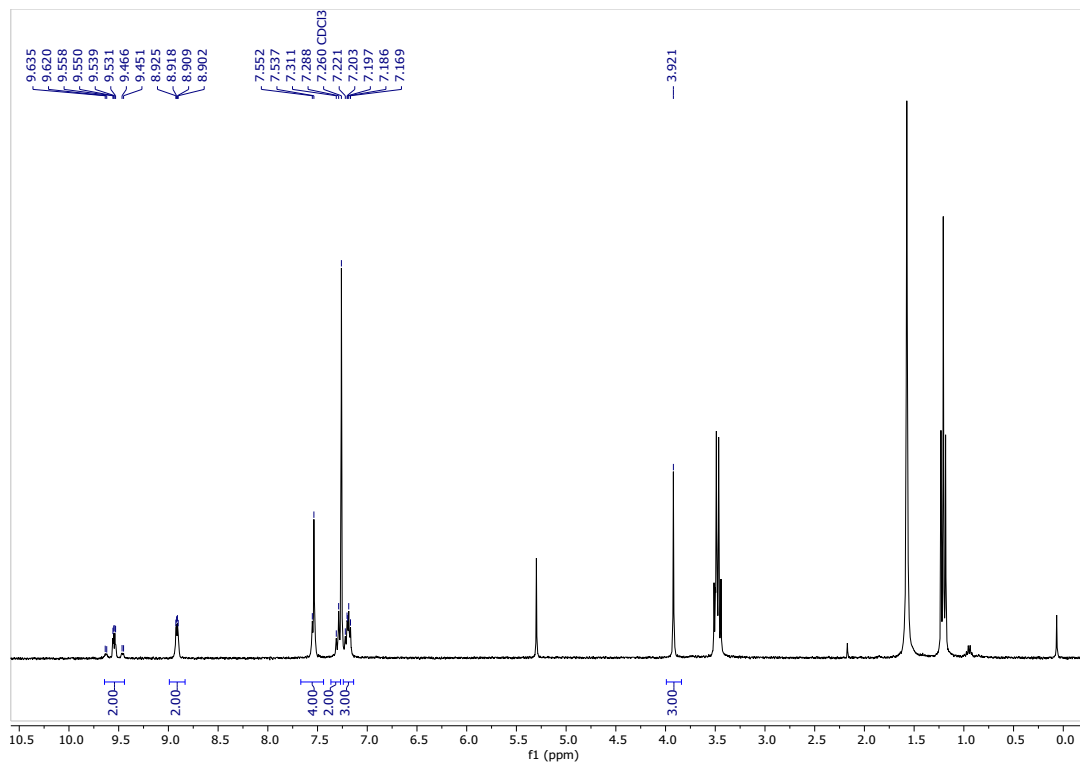
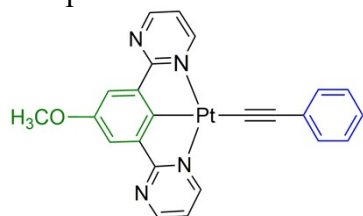


Fig. S8 ¹H NMR spectrum (300 MHz, CDCl₃) of 7.

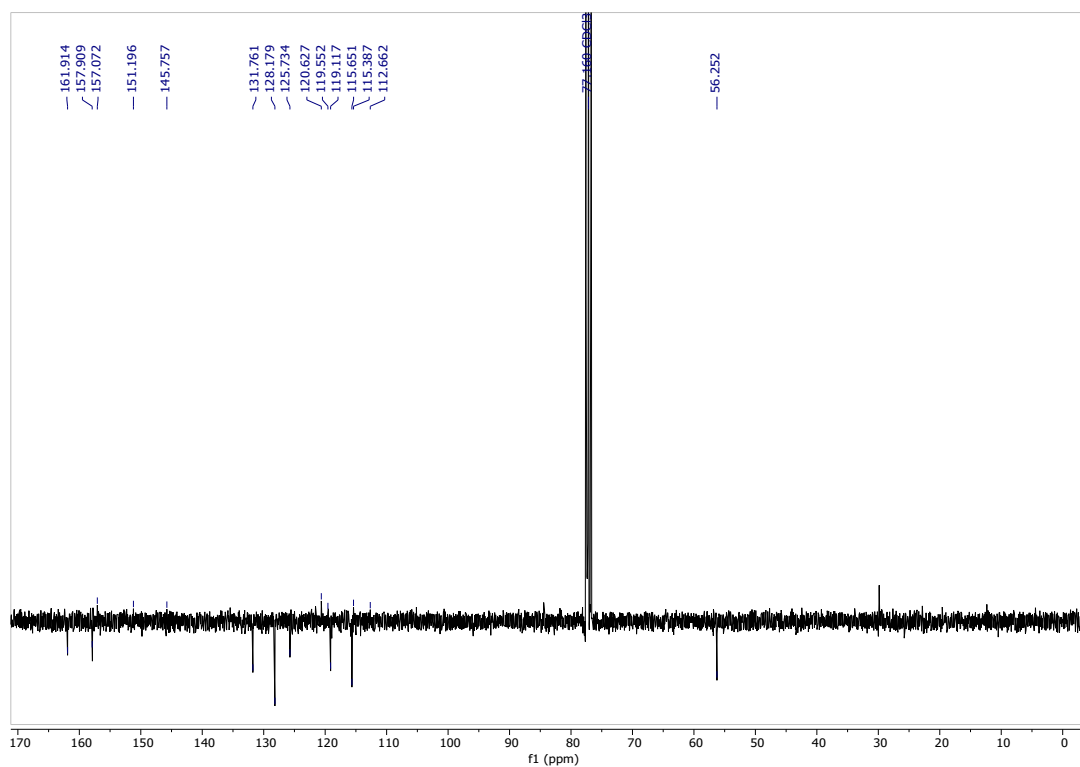


Fig. S9 ¹³C NMR spectrum (JMOD, 75 MHz, CDCl₃) of 7.

Complex 8

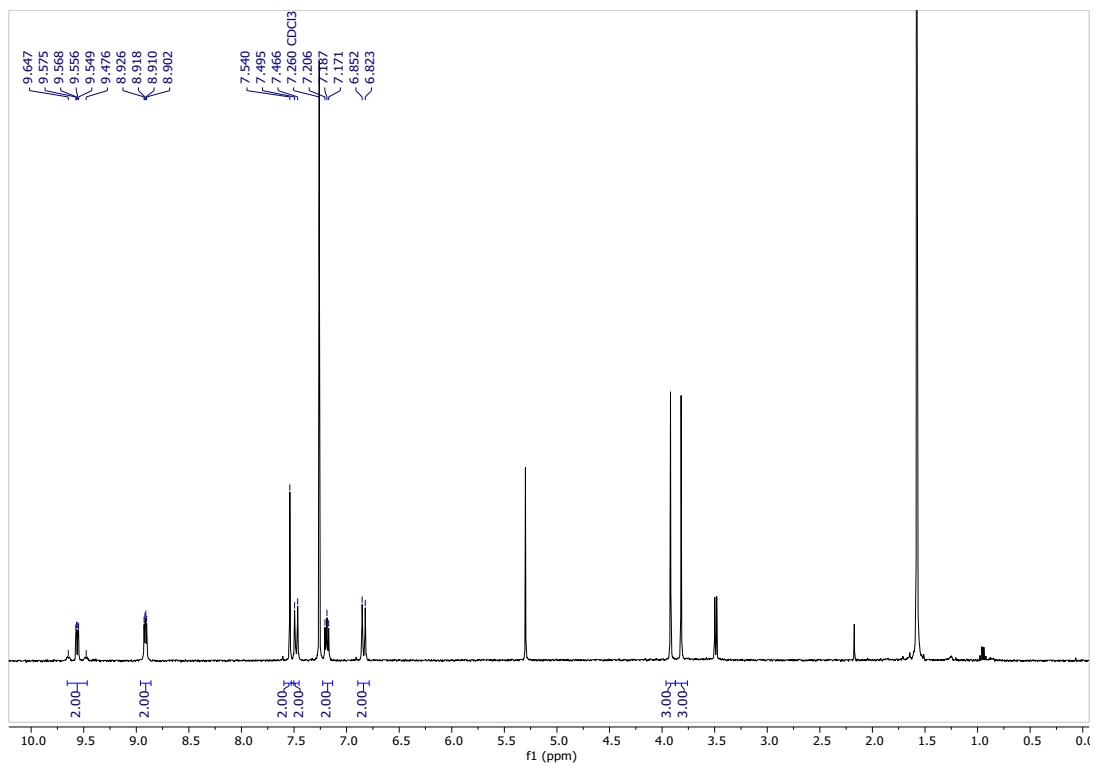
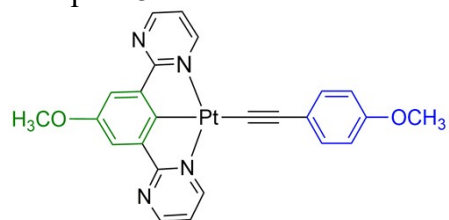


Fig. S10 ¹H NMR spectrum (300 MHz, CDCl₃) of 8.

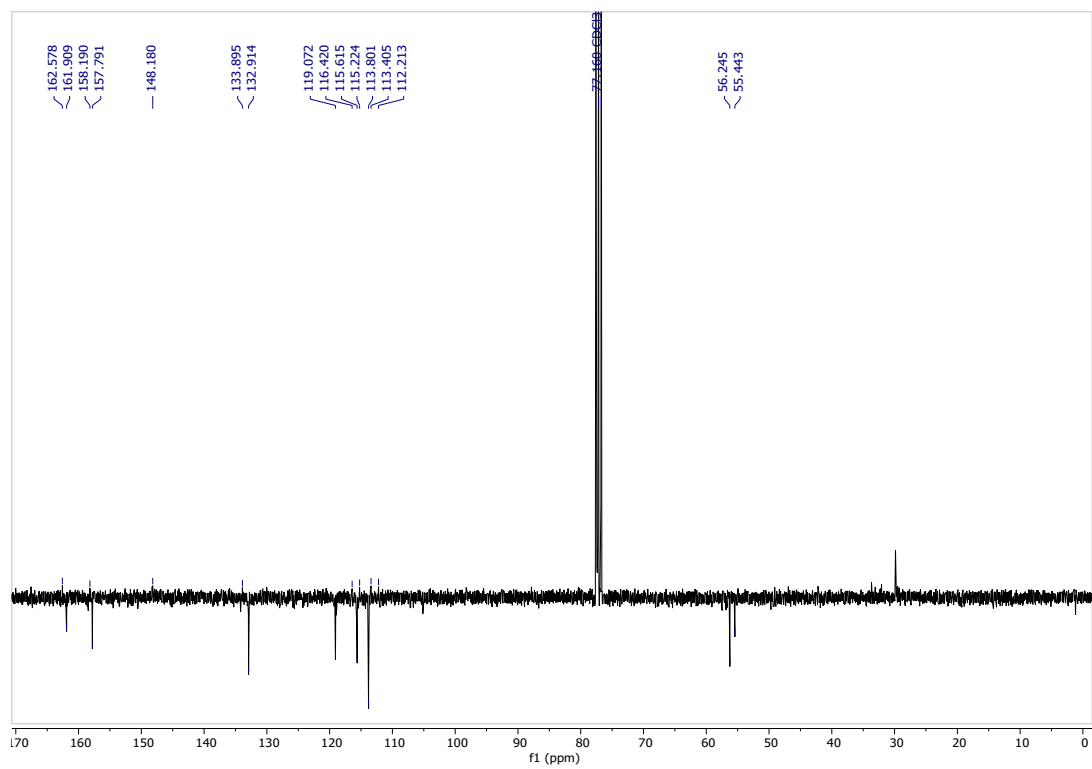


Fig. S11 ¹³C NMR spectrum (JMOD, 75 MHz, CDCl₃) of 8.

Complex 9

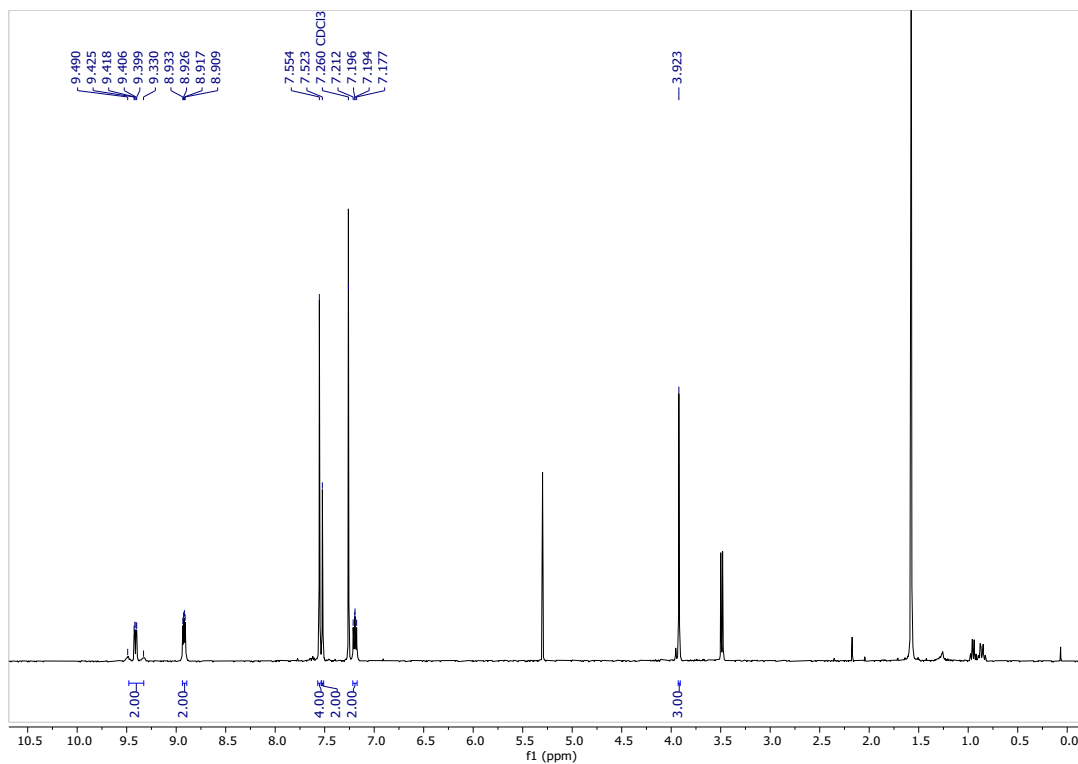
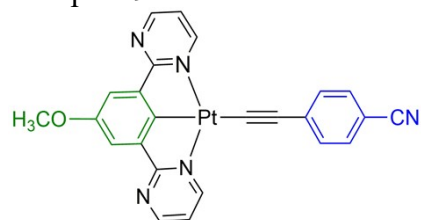


Fig. S12 ^1H NMR spectrum (300 MHz, CDCl_3) of 9.

Complex **10**

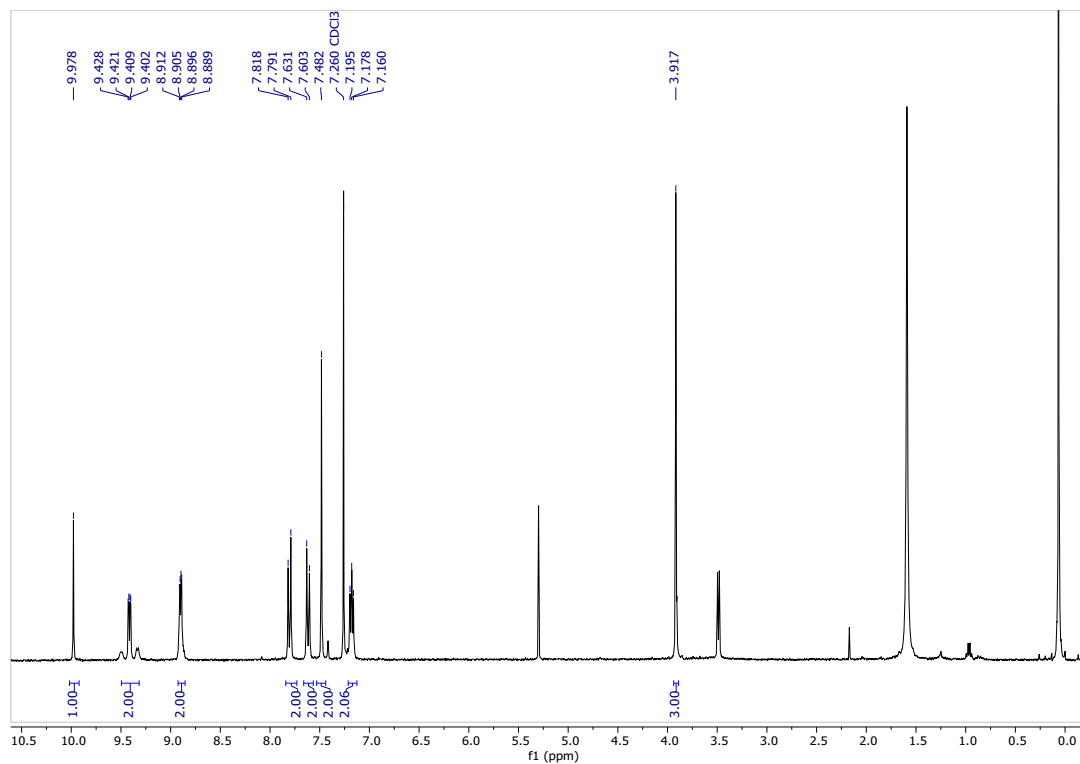
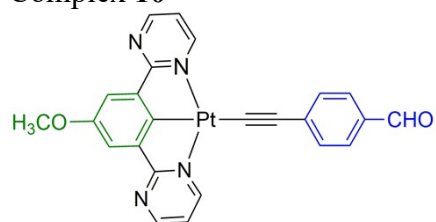


Fig. S13 ¹H NMR spectrum (300 MHz, CDCl₃) of **10**.

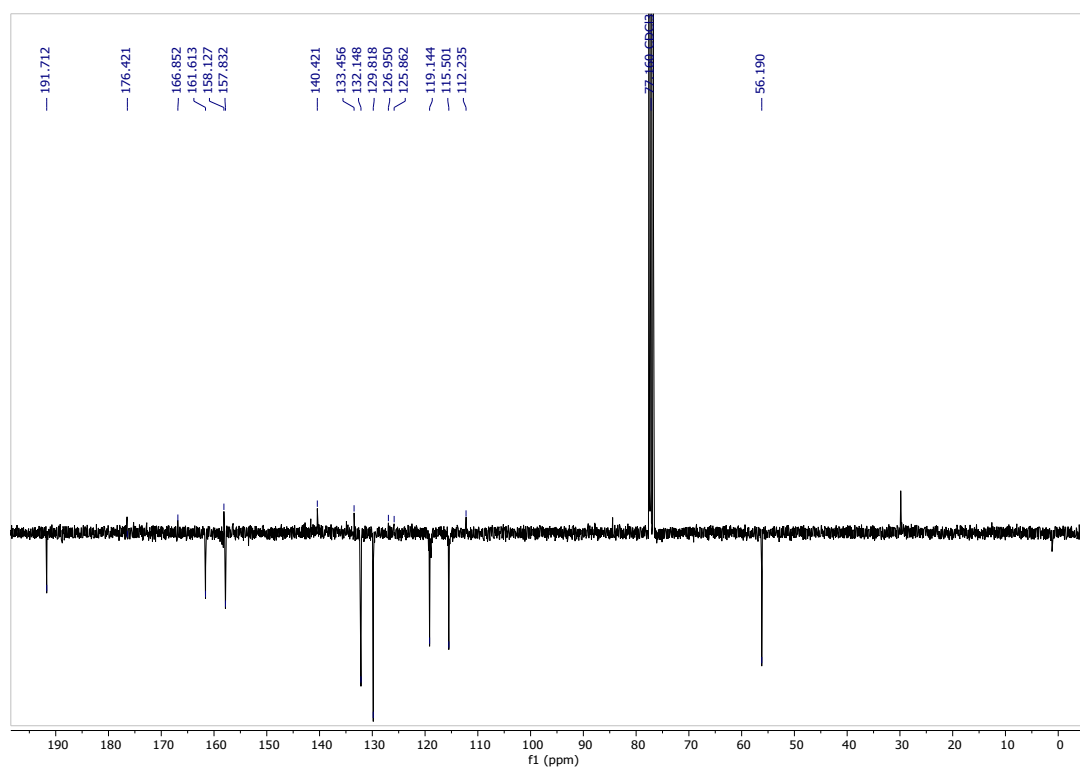


Fig. S14 ¹³C NMR spectrum (JMOD, 75 MHz, CDCl₃) of **10**.

Complex 11

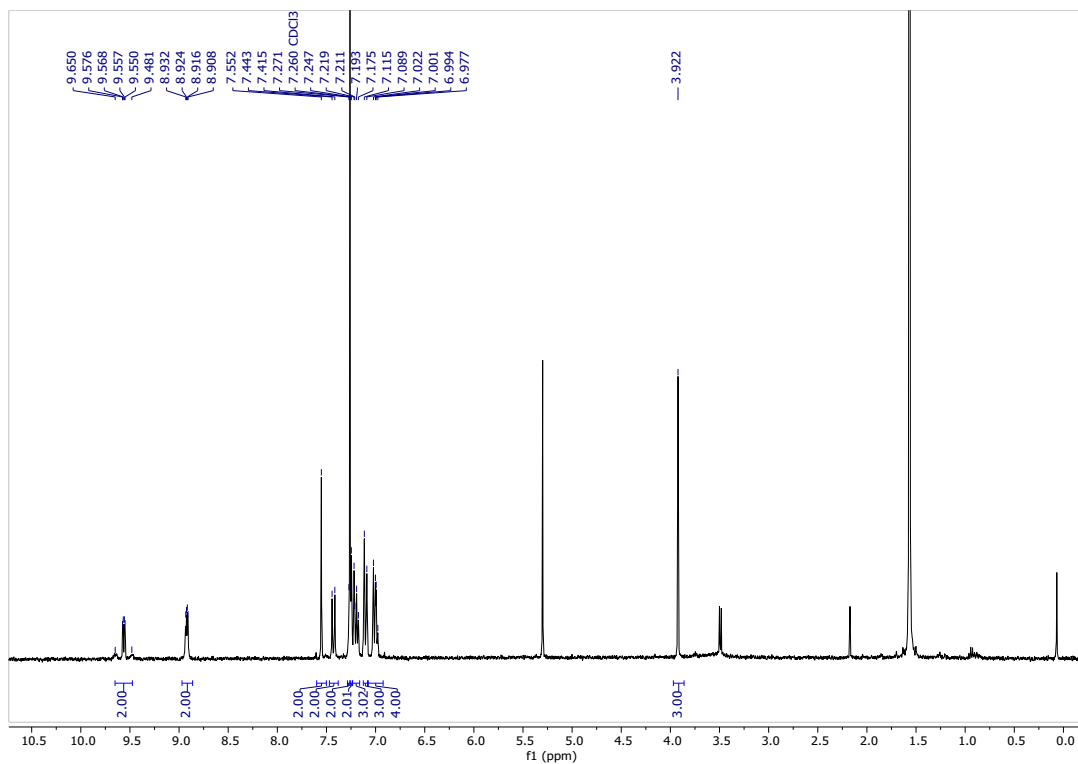
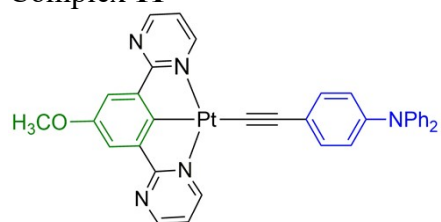


Fig. S15 ¹H NMR spectrum (300 MHz, CDCl₃) of 11.

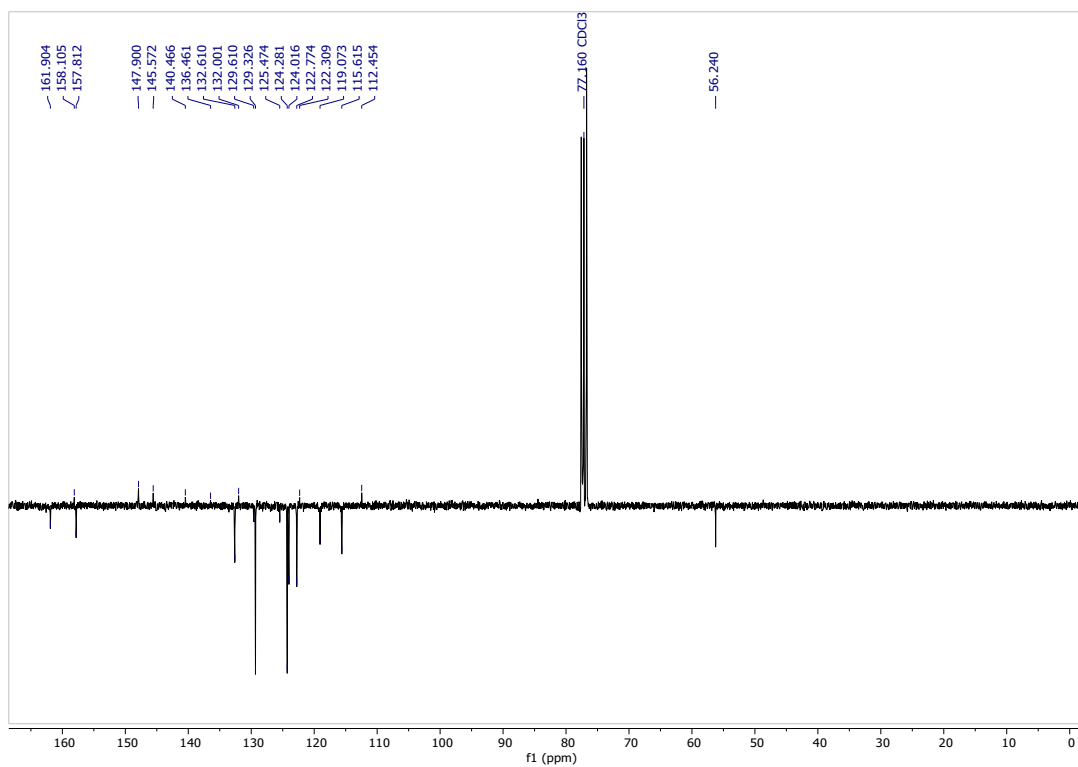


Fig. S16 ¹³C NMR spectrum (JMOL, 75 MHz, CDCl₃) of 11.

Complex 12

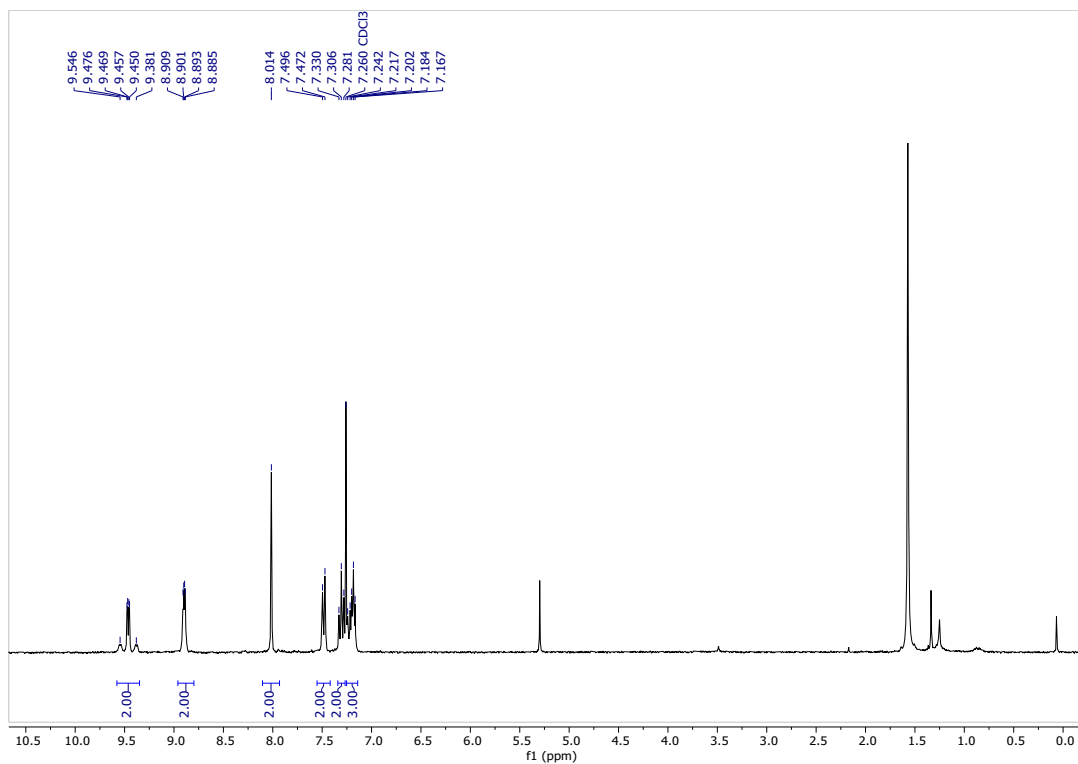
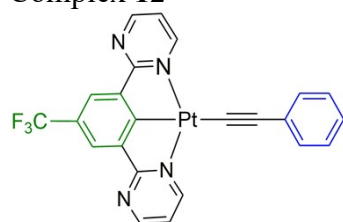


Fig. S17 ¹H NMR spectrum (300 MHz, CDCl₃) of 12.

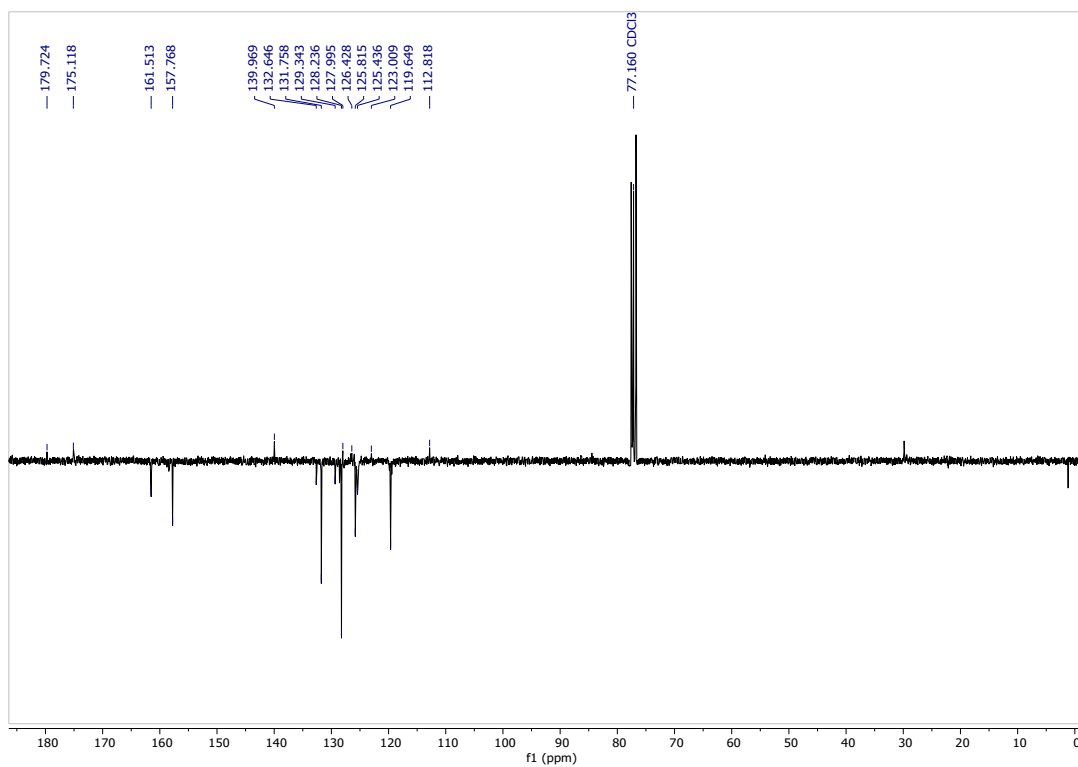


Fig. S18 ¹³C NMR spectrum (JMOD, 75 MHz, CDCl₃) of 12.

Complex 13

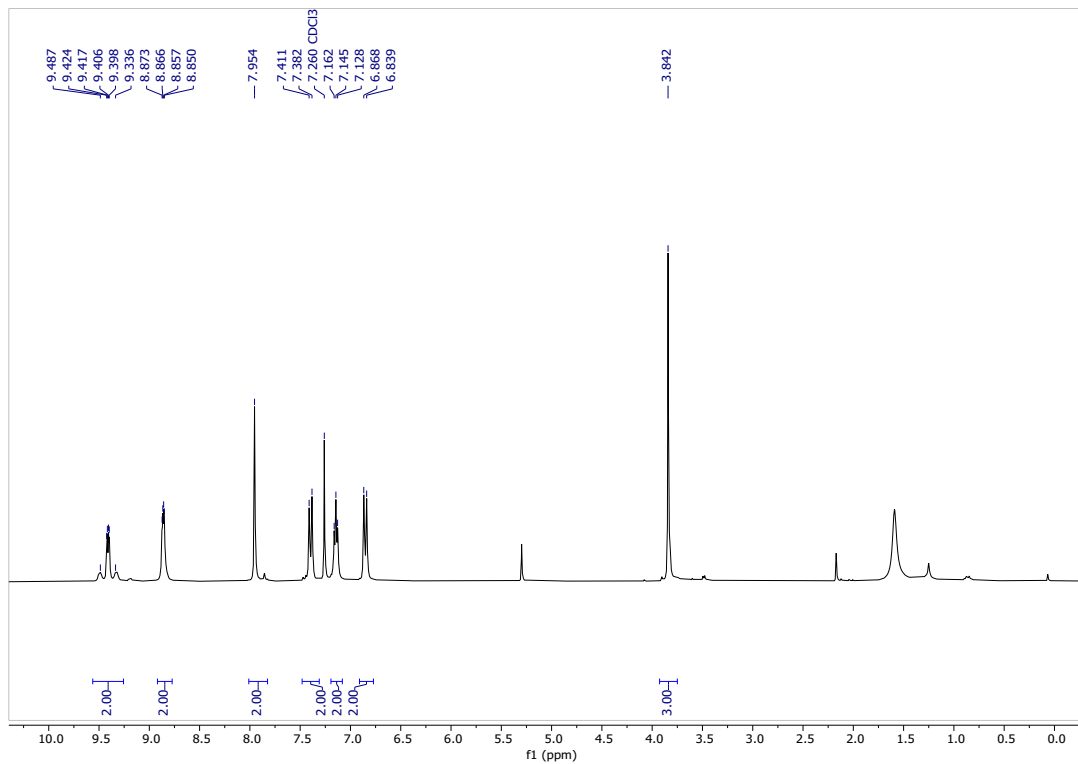
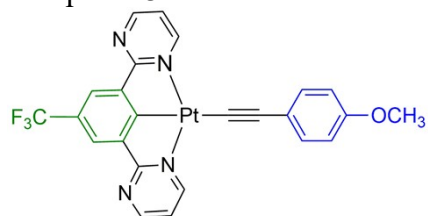


Fig. S19 ^1H NMR spectrum (300 MHz, CDCl_3) of 13.

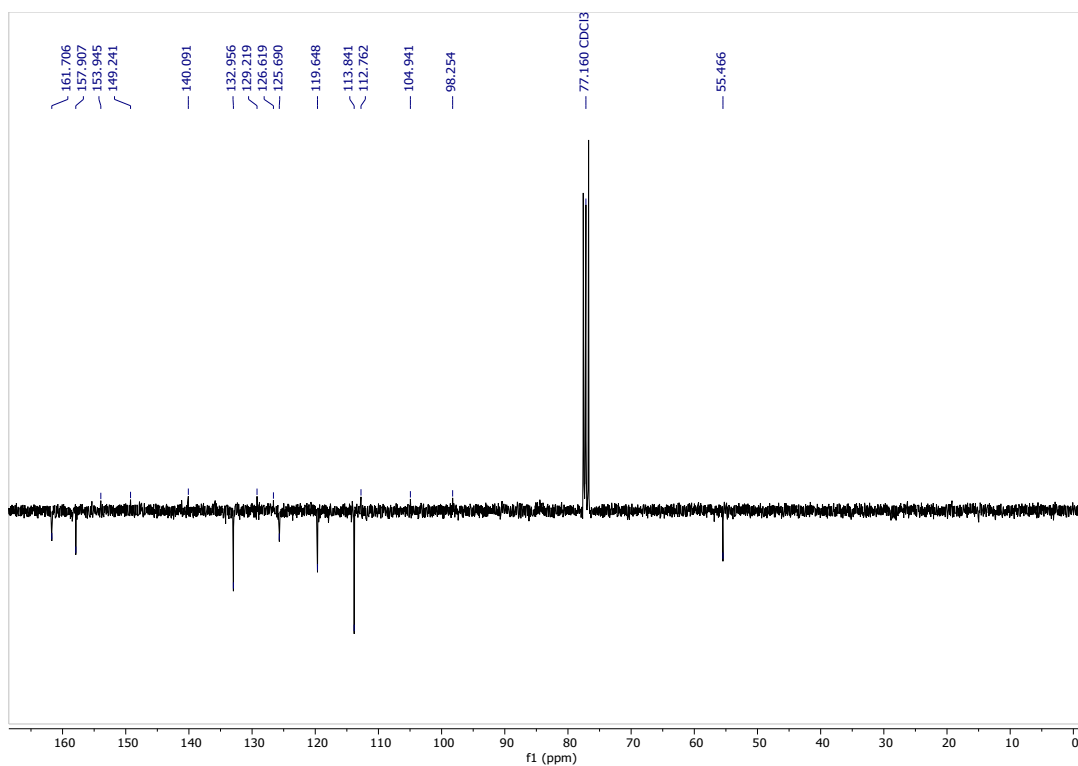


Fig. S20 ^{13}C NMR spectrum (JMOD, 75 MHz, CDCl_3) of 13.

Complex 14

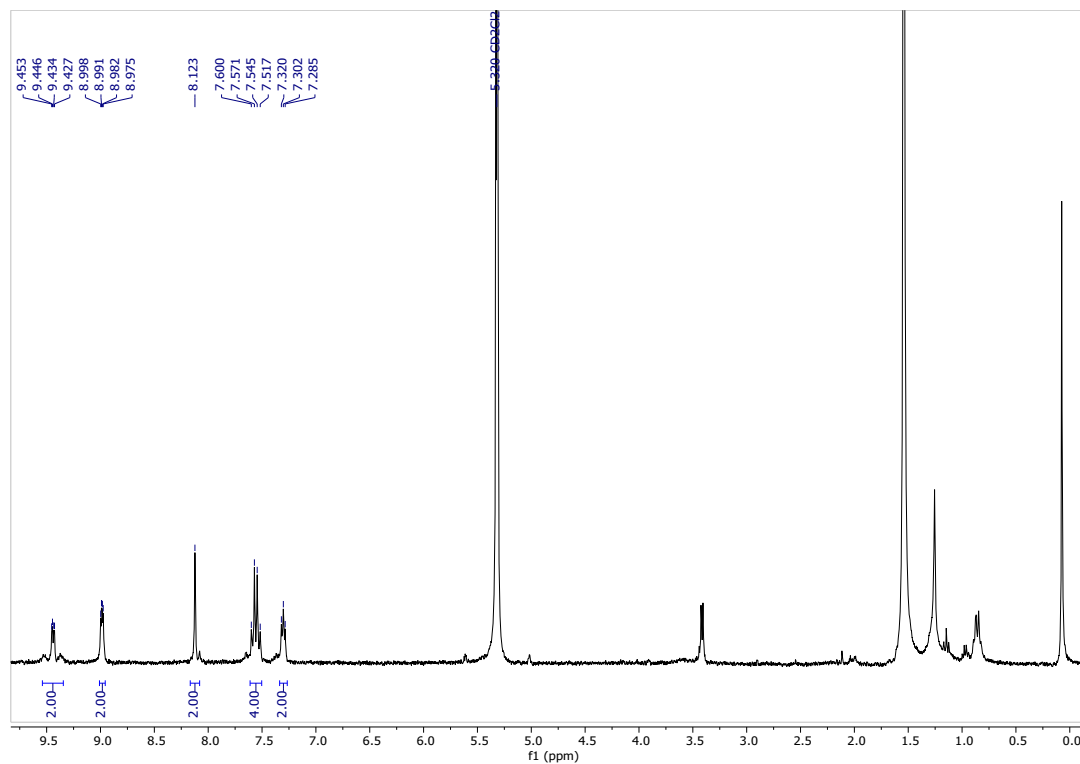
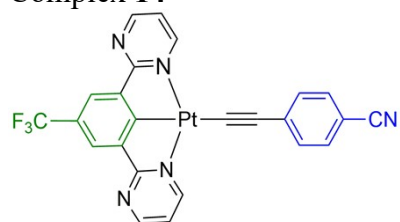
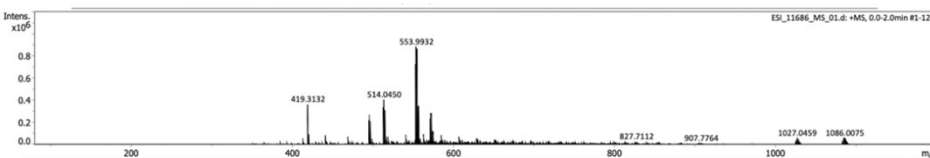
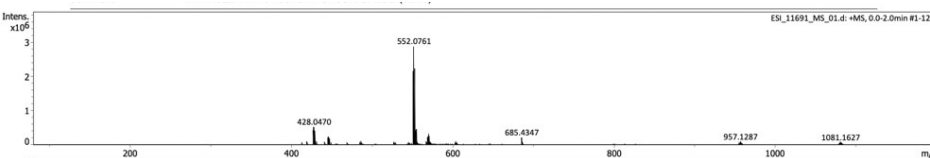
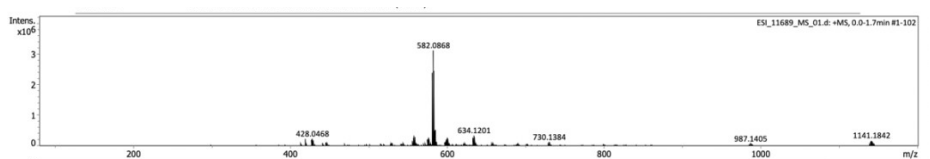
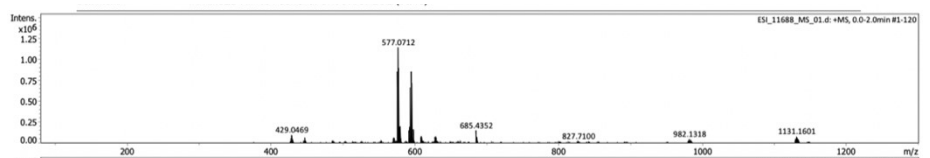
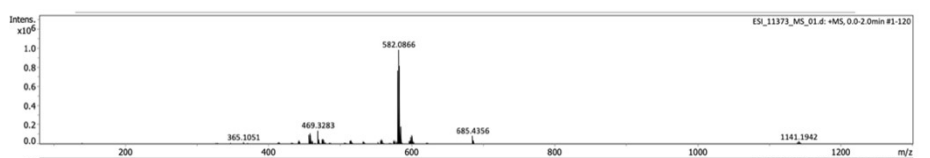
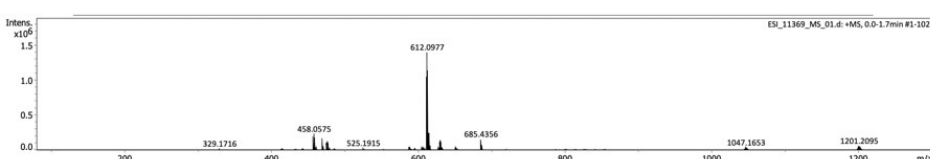
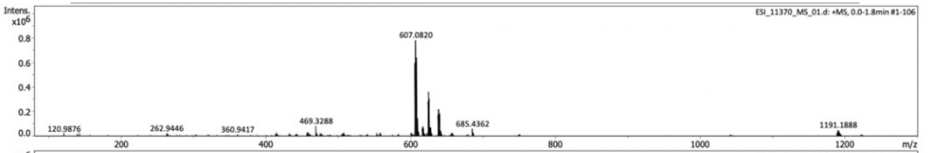
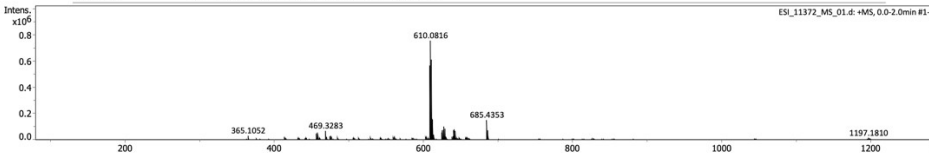
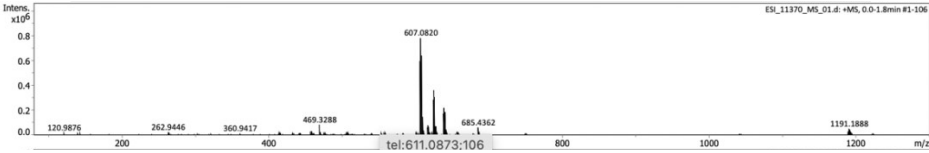
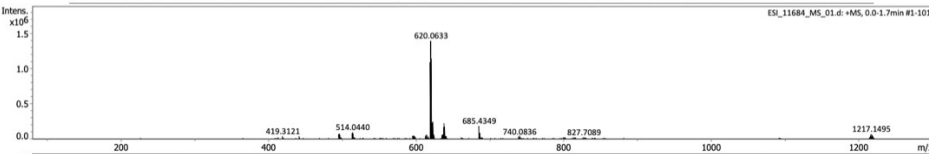
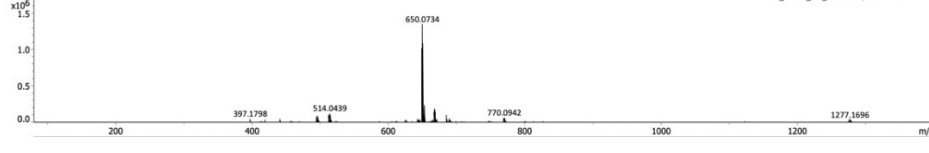
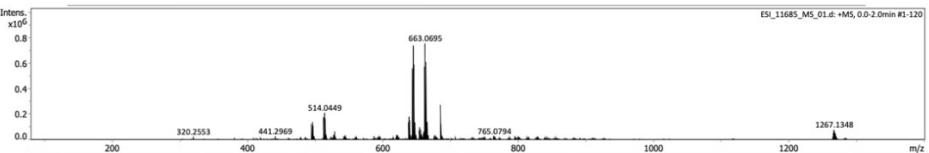
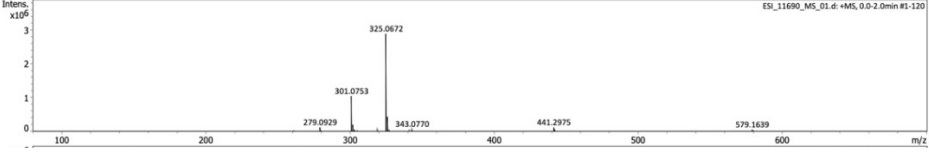


Fig. S21 ¹H NMR spectrum (300 MHz, CDCl₃) of 14.

Table S1. Mass spectra ESI-MS (CH₃OH/CH₂Cl₂ : 90/10) of complexes **3-14** and ligand **20**

| No | Mass Spectra | Assignment (m/z values) |
|----|--|---|
| 3 |  | <p>[M+Na]⁺(C₁₅H₈N₄F₃³⁵ClNa¹⁹⁵Pt) 553.9930, found: 553.9932 (0 ppm) [M₂+Na]⁺(C₁₅H₁₀N₄OF₃³⁵ClNa¹⁹⁵Pt) 572.0035, found: 572.0034 (0 ppm) [M·Cl]⁺(C₁₅H₈N₄F₃¹⁹⁵Pt) 496.0343, found: 496.0343 (0 ppm)</p> |
| 4 |  | <p>[M+Na]⁺(C₂₂H₁₄N₄Na¹⁹⁵Pt) 552.0759, found: 552.0761 (0 ppm) [M₂+Na]⁺(C₂₂H₁₆N₄ONa¹⁹⁵Pt) 570.0064, found: 570.0060 (1 ppm) [M·C₈H₅]⁺(C₁₄H₉N₄¹⁹⁵Pt) 428.0470, found: 428.0470 (0 ppm)</p> |
| 5 |  | <p>[M+Na]⁺(C₂₃H₁₆N₄ONa¹⁹⁵Pt) 582.0864, found: 582.868 (1 ppm) [M₂+Na]⁺(C₂₃H₁₈N₄¹⁶ONa¹⁹⁵Pt) 600.0969, found: 600.0065 (1 ppm) [M·C₉H₇O]⁺(C₁₄H₉N₄¹⁹⁵Pt) 428.0469, found: 428.0468 (0 ppm)</p> |
| 6 |  | <p>[M+Na]⁺(C₂₃H₁₃N₅Na¹⁹⁵Pt) 577.0711, found: 577.0712 (0 ppm) [M₂+Na]⁺(C₂₃H₁₅N₅ONa¹⁹⁵Pt) 595.0816, found: 595.0816 (0 ppm) [M·C₉H₄N]⁺(C₁₄H₉N₄¹⁹⁵Pt) 428.0469, found: 428.0468 (0 ppm)</p> |
| 7 |  | <p>[M+Na]⁺(C₂₃H₁₆N₄ONa¹⁹⁵Pt) 582.0864, found: 577.0666 (0 ppm) [M·C₈H₅]⁺(C₁₅H₁₁N₄O¹⁹⁵Pt) 458.0575 found: 458.0570 (1 ppm) [M+K]⁺(C₂₃H₁₆N₄OK¹⁹⁵Pt) 598.0603 found: 598.0599 (1 ppm) [M₂+Na]⁺(C₂₃H₁₈N₄O₂Na¹⁹⁵Pt) 600.0969 found: 600.0963 (1 ppm) M⁺ (m/z 559); [M+H]⁺ (m/z 560), [L₂Pt₂]⁺ (m/z 558, 660,916); [L₂Pt₂L]⁺ (m/z 1017 base peak, 1118,1219, 1368)</p> |
| 8 |  | <p>[M+Na]⁺(C₂₄H₁₈N₄O₂Na¹⁹⁵Pt) 612.0970, found: 612.0977 (1 ppm) [M·C₉H₇O]⁺(C₁₅H₁₁N₄O¹⁹⁵Pt) 458.0575 found: 458.055 (0 ppm) [M₂+Na]⁺(C₂₄H₂₀N₄O₃Na¹⁹⁵Pt) 630.1075 found: 630.1075 (1 ppm) M⁺ (m/z 589); [M+H]⁺ (m/z 590), [L₂Pt₂]⁺ (m/z 916); [L₂Pt₂L]⁺ (m/z 1047 base peak)</p> |

| | | |
|----|--|---|
| 9 |  | <p>[M+Na]⁺(C₂₄H₁₅N₅O₂Na¹⁹⁵Pt) 607.0817, found: 607.0820 (0 ppm)</p> <p>[M₂+Na]⁺(C₂₄H₁₇N₅O₂Na¹⁹⁵Pt) 625.0922 found: 625.0925 (0 ppm)</p> <p>[M₃+Na]⁺(C₂₅H₁₉N₅O₂Na¹⁹⁵Pt) 639.1079 found: 639.1079 (0 ppm)</p> <p>[M₃+H]⁺(C₂₅H₂₀N₅O₂¹⁹⁵Pt) 617.1259 found: 617.1259 (0 ppm)</p> <p>M⁺ (m/z 584); [M+H]⁺ (m/z 585), [LPt]⁺ (m/z 458); [L₂Pt₂L]⁺ (m/z 1042 base peak, 1074)</p> |
| 10 |  | <p>[M+Na]⁺(C₂₄H₁₆N₄O₂Na¹⁹⁵Pt) 610.0813, found: 610.0816 (0 ppm)</p> <p>[M₂+Na]⁺(C₂₄H₁₈N₄O₃Na¹⁹⁵Pt) 628.0919 found: 628.0907 (2 ppm)</p> <p>[M₃+Na]⁺(C₂₅H₂₀N₄O₃Na¹⁹⁵Pt) 642.1075 found: 642.1066 (2 ppm) M⁺ (m/z 587); [LPt]⁺ (m/z 458.); [L₂Pt₂L]⁺ (m/z 708,716,837,916), [L₂Pt₂L]⁺ (m/z 1045 base peak, 1173)</p> |
| 11 |  | <p>[M+Na]⁺(C₃₅H₂₅N₅O₂Na¹⁹⁵Pt) 749.6000, found 749.1603 (0 ppm) [M- C₂₀H₁₄N]⁺(C₁₅H₁₁N₄O¹⁹⁵Pt) 458.0575 found: 458.0579 (1 ppm)</p> <p>[M₂+Na]⁺(C₃₅H₂₇N₅O₂Na¹⁹⁵Pt) 767.1704 found: 767.1793 (2 ppm) M⁺ (m/z 726); [L₂Pt₂L]⁺ (m/z 916), [L₂Pt₂L]⁺ (m/z 101184 base peak)</p> |
| 12 |  | <p>[M+Na]⁺(C₂₃H₁₃N₄F₃Na¹⁹⁵Pt) 620.0632, found: 620.0633 (0 ppm)</p> <p>[M+K]⁺(C₂₃H₁₃N₄F₃K¹⁹⁵Pt) 636.0371 found: 636.0365 (1 ppm)</p> <p>[M₂+Na]⁺(C₂₃H₁₅N₄OF₃Na¹⁹⁵Pt) 638.0738 found: 638.0732 (1 ppm)</p> <p>[M-C₈H₅]⁺(C₁₅H₈N₄F₃¹⁹⁵Pt) 496.0343 found: 496.0334 (2 ppm)</p> |
| 13 |  | <p>[M+Na]⁺(C₂₄H₁₅N₄O₂F₃Na¹⁹⁵Pt) 650.0738, found: 650.0734 (1 ppm)</p> <p>[M₂+Na]⁺(C₂₄H₁₇N₄O₂F₃Na¹⁹⁵Pt) 688.0843 found: 688.0833 (2 ppm)</p> <p>[M₃+Na]⁺(C₃₁H₁₉N₄O₃F₃Na¹⁹⁵Pt) 770.0949 found: 770.0942 (1 ppm)</p> |
| 14 |  | <p>[M+Na]⁺(C₂₄H₁₂N₅F₃Na¹⁹⁵Pt) 645.0585, found: 645.0590 (1 ppm)</p> <p>[M₂+Na]⁺(C₂₄H₁₄N₅OF₃Na¹⁹⁵Pt) 663.0691 found: 663.0695 (1 ppm)</p> <p>[M-C₉H₄N]⁺(C₁₅H₈N₄F₃¹⁹⁵Pt) 496.0343 found: 496.0339 (1 ppm)</p> |
| 20 |  | <p>[M+Na]⁺(C₁₅H₉N₄F₃Na) 325.0673, found: 325.0672 (0 ppm)</p> |

Crystallographic Data for 7 and 8

Complex 7: crystal Data for $C_{23}H_{16}N_4O$ Pt, ($M = 559.49$), monoclinic, space group $C 2/c$ (I.T.#15), $a = 24.768(3)$, $b = 10.8889(13)$, $c = 13.8726(19)\text{\AA}$, $\beta = 92.343(6)^\circ$, $V = 3738.3(8)\text{\AA}^3$. $Z = 8$, $d = 1.988\text{ g.cm}^{-3}$, $\mu = 7.530\text{ mm}^{-1}$. The structure was solved by dual-space algorithm using the *SHELXT* program,^[1] and then refined with full-matrix least-square methods based on F^2 (*SHELXL*).^[2] All non-hydrogen atoms were refined with anisotropic atomic displacement parameters. H atoms were finally included in their calculated positions. A final refinement on F^2 with 4245 unique intensities and 221 parameters converged at $\omega R(F^2) = 0.0965$ ($R(F) = 0.0467$) for 2978 observed reflections with $I > 2\sigma(I)$.

Table S2. Crystallographic data for 7.

| | | |
|--------------------------------------|---|---------------------------|
| Compound | 7 | |
| Empirical formula | C ₂₃ H ₁₆ N ₄ O Pt | |
| CCDC | 2126978 | |
| Formula weight | 559.49 | |
| Temperature | 150 K | |
| Wavelength | 0.71073 Å | |
| Crystal system | Monoclinic | |
| Space group | $C 2/c$ | |
| Unit cell dimensions | $a = 24.768(3)\text{\AA}$ | $\alpha = 90^\circ$ |
| | $b = 10.8889(13)\text{\AA}$ | $\beta = 92.343(6)^\circ$ |
| | $c = 13.8726(19)\text{\AA}$ | $\gamma = 90^\circ$ |
| Volume | $3738.3(8)\text{\AA}^3$ | |
| Z | 8 | |
| Density (calculated) | 1.988 g/cm^3 | |
| Absorption coefficient | 7.530 mm^{-1} | |
| F(000) | 2144 | |
| Crystal size | 0.160 x 0.150 x 0.130 mm | |
| Crystal color | orange | |
| Theta range for data collection | 2.497 to 27.473°. | |
| Index ranges | -22 ≤ h ≤ 31, -14 ≤ k ≤ 14, -16 ≤ l ≤ 17 | |
| Reflections collected | 12914 | |
| Independent reflections | 4245 [R(int) = 0.0636] | |
| Reflections [$I > 2\sigma(I)$] | 2978 | |
| Completeness to theta max | 99.0 % | |
| Absorption correction | multi-scan | |
| Max. and min. transmission | 0.376 and 0.297 | |
| Refinement method | Full-matrix least-squares on F^2 | |
| Data / restraints / parameters | 4245 / 1 / 221 | |
| Goodness-of-fit on F^2 | 1.031 | |
| Final R indices [$I > 2\sigma(I)$] | R1 = 0.0467, wR2 = 0.0965 | |
| R indices (all data) | R1 = 0.0773, wR2 = 0.1078 | |
| Largest diff. peak and hole | 2.575 and -1.931 e.Å ⁻³ | |

Complex 8: crystal Data for C₂₄ H₁₈ N₄ O₂ Pt, (*M* = 589.51), monoclinic, space group *P* 2₁/*c* (I.T.#14), *a* = 12.4772(12), *b* = 7.8562(5), *c* = 20.3724(18) Å, $\alpha = 90$, $\beta = 94.458(6)$, $\gamma = 90$ °, *V* = 1990.9(3) Å³. *Z* = 4, *d* = 1.967 g.cm⁻³, $\mu = 7.078$ mm⁻¹. The structure was solved by dual-space algorithm using the SHELXT program,^[1] and then refined with full-matrix least-square methods based on *F*² (SHELXL).^[2] All non-hydrogen atoms were refined with anisotropic atomic displacement parameters. H atoms were finally included in their calculated positions. A final refinement on *F*² with 3675 unique intensities and 282 parameters converged at $\omega R(F^2) = 0.0852$ (*R*(*F*) = 0.0424) for 2555 observed reflections with *I* > 2 σ (*I*).

Table S3. Crystallographic data for **8**.

| | | |
|--|--|-----------------------------|
| Compound | 8 | |
| Empirical formula | C ₂₄ H ₁₈ N ₄ O ₂ Pt | |
| CCDC | 2126979 | |
| Formula weight | 589.51 | |
| Temperature | 150 K | |
| Wavelength | 0.71073 Å | |
| Crystal system | Monoclinic | |
| Space group | <i>P</i> 2 ₁ / <i>c</i> | |
| Unit cell dimensions | <i>a</i> = 12.4772(12) Å | $\alpha = 90^\circ$. |
| | <i>b</i> = 7.8562(5) Å | $\beta = 94.458(6)^\circ$. |
| | <i>c</i> = 20.3724(18) Å | $\gamma = 90^\circ$. |
| Volume | 1990.9(3) Å ³ | |
| <i>Z</i> | 4 | |
| Density (calculated) | 1.967 g/cm ³ | |
| Absorption coefficient | 7.078 mm ⁻¹ | |
| <i>F</i> (000) | 1136 | |
| Crystal size | 0.230 x 0.090 x 0.040 mm | |
| Crystal color | orange | |
| Theta range for data collection | 2.686 to 25.681°. | |
| Index ranges | -16 ≤ <i>h</i> ≤ 16, 0 ≤ <i>k</i> ≤ 10, 0 ≤ <i>l</i> ≤ 26 | |
| Reflections collected | 3675 | |
| Independent reflections | 3675 [<i>R</i> (int) = 0.0903] | |
| Reflections [<i>I</i> > 2 σ (<i>I</i>)] | 2555 | |
| Completeness to theta max | 97.1 % | |
| Absorption correction | multi-scan | |
| Max. and min. transmission | 0.753 and 0.410 | |
| Refinement method | Full-matrix least-squares on <i>F</i> ² | |
| Data / restraints / parameters | 3675 / 0 / 282 | |
| Goodness-of-fit on <i>F</i> ² | 0.949 | |
| Final <i>R</i> indices [<i>I</i> > 2 σ (<i>I</i>)] | <i>R</i> 1 = 0.0424, <i>wR</i> 2 = 0.0852 | |
| <i>R</i> indices (all data) | <i>R</i> 1 = 0.0778, <i>wR</i> 2 = 0.0930 | |
| Largest diff. peak and hole | 1.446 and -1.360 e.Å ⁻³ | |

Additional Cyclic Voltammetry

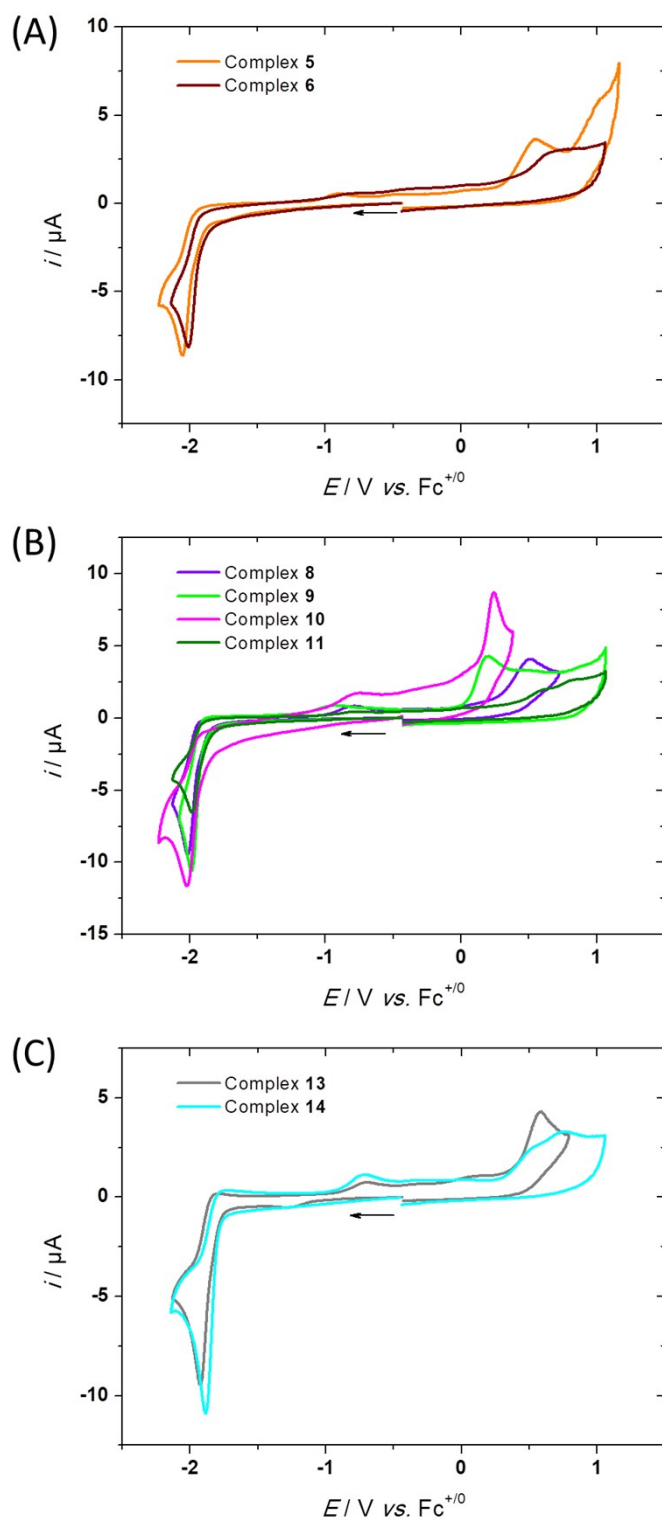


Fig. S22 Cyclic voltammograms at a Pt working electrode ($E / \text{V vs. Fc}^{+}/\text{Fc}$) of A) complexes **5** (orange) and **6** (brown); B) complexes **8** (purple), **9** (light green), **10** (pink) and **11** (olive); C) complexes **13** (gray) and **14** (cyan), in $\text{CH}_2\text{Cl}_2/\text{NBu}_4\text{PF}_6$ 0.1 M under inert atmosphere. $C = 0.5 \text{ mM}$.

Additional Photophysical Data

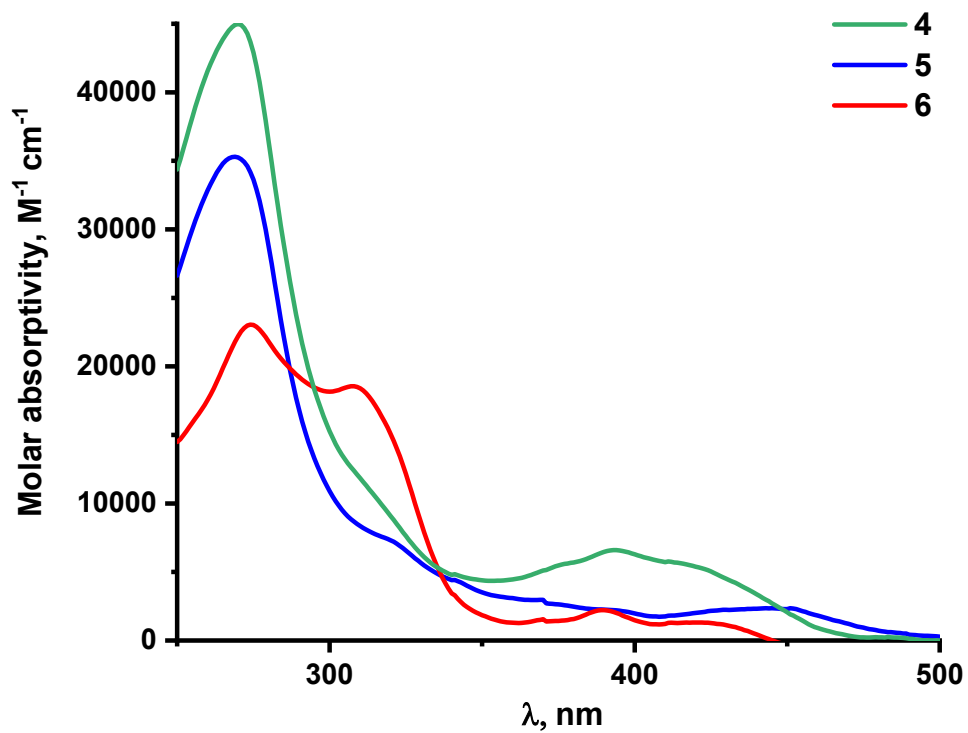


Fig. S23 Absorption spectra of complexes 4-6 in CH₂Cl₂ (C ~ 10⁻⁵ M).

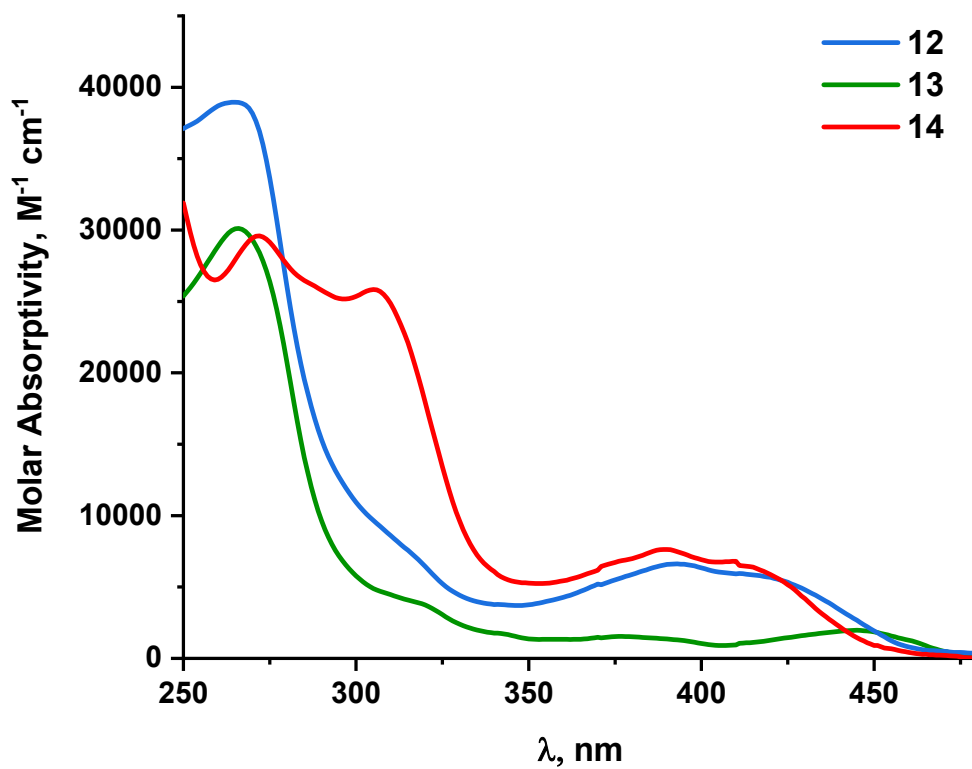


Fig. S24 Absorption spectra of complexes 12-14 in CH₂Cl₂ (C ~ 10⁻⁵ M).

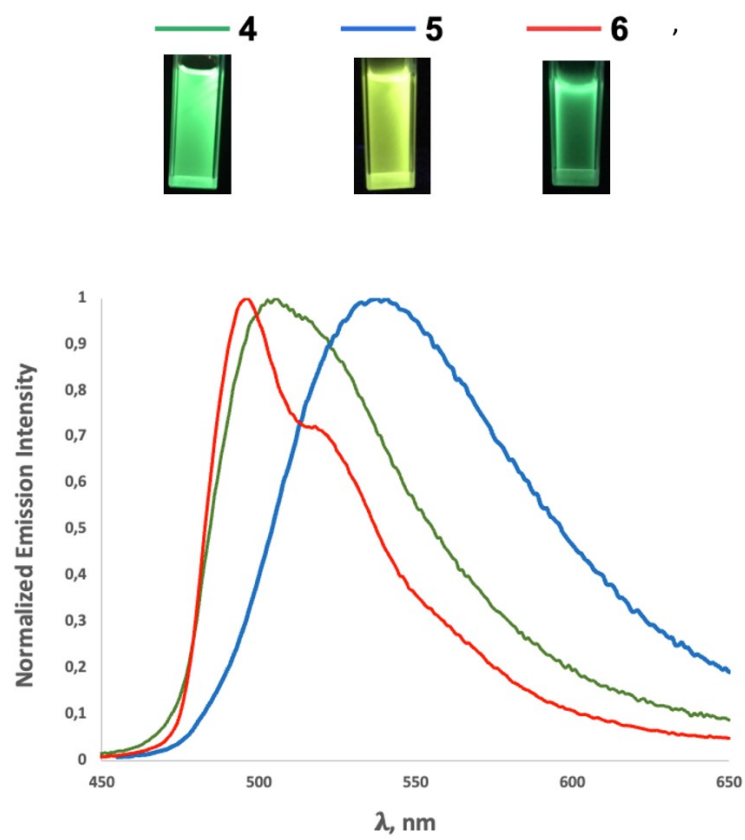


Fig. S25 Normalized emission spectra of complexes **4-6** in deoxygenated CH_2Cl_2 solution ($C \sim 10^{-5}$ M). $\lambda_{\text{exc}} = \lambda_{\text{abs}}^{\text{max}}$ of the lowest energy band Inset: picture of CH_2Cl_2 solution taken under UV irradiation.

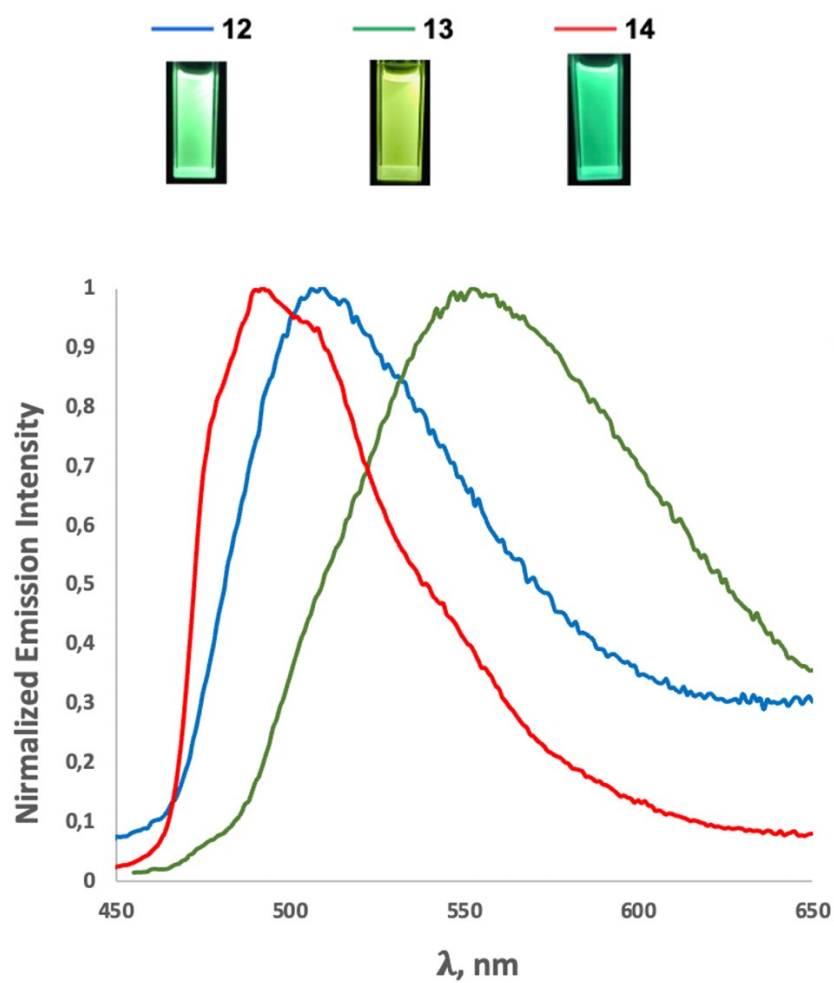


Fig. S26 Normalized emission spectra of complexes **12-14** in deoxygenated CH_2Cl_2 solution ($C \sim 10^{-5}$ M). $\lambda_{\text{exc}} = \lambda_{\text{max}}^{\text{abs}}$ of the lowest energy band Inset: picture of CH_2Cl_2 solution taken under UV irradiation.

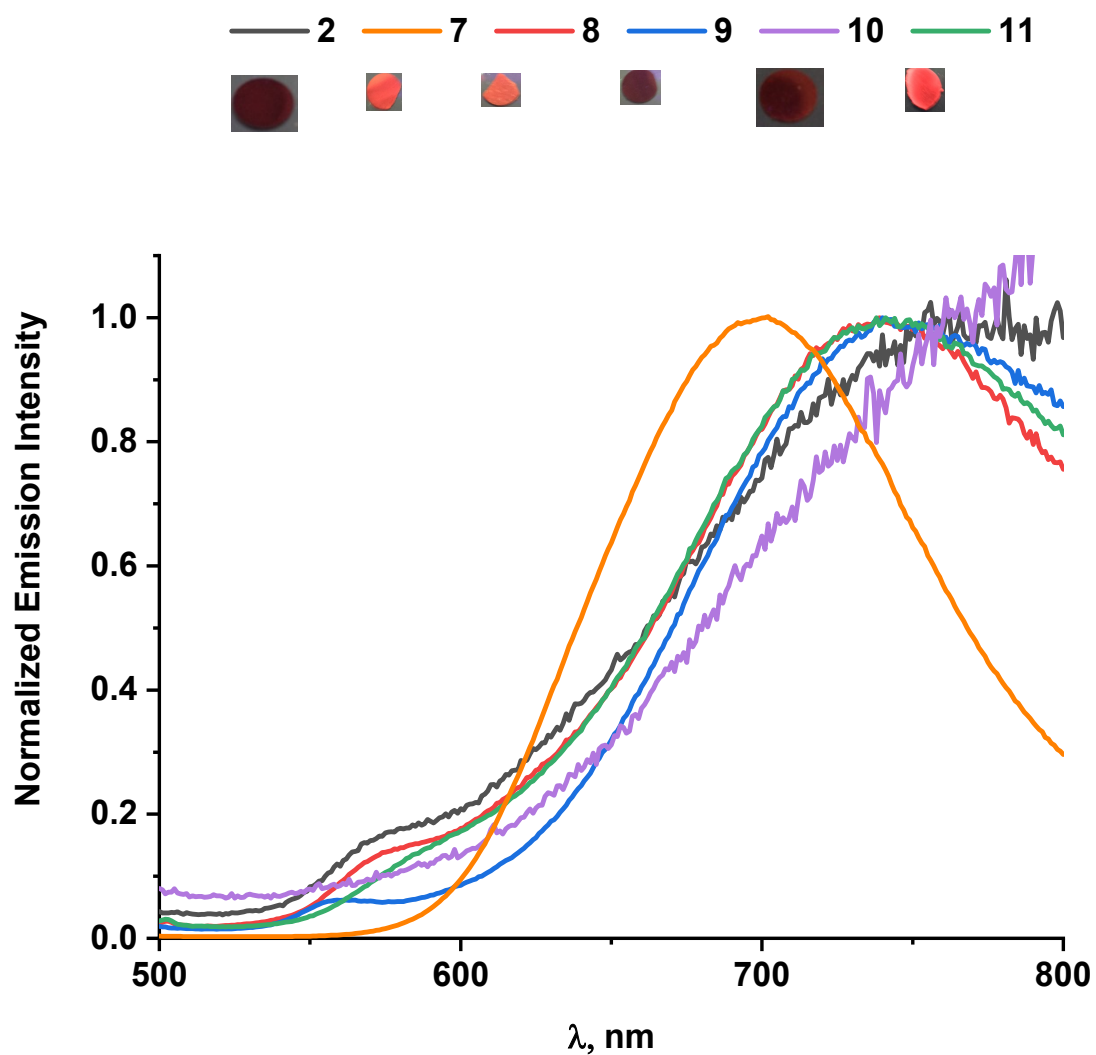


Fig. S27 Normalized emission spectra of complexes **2**, and **7-11** in KBr matrix (2 w%). $\lambda_{\text{exc}} = \lambda_{\text{max}}^{\text{abs}}$ of the lowest energy band in CH_2Cl_2 solution. Inset: picture of KBr pellets taken under UV irradiation

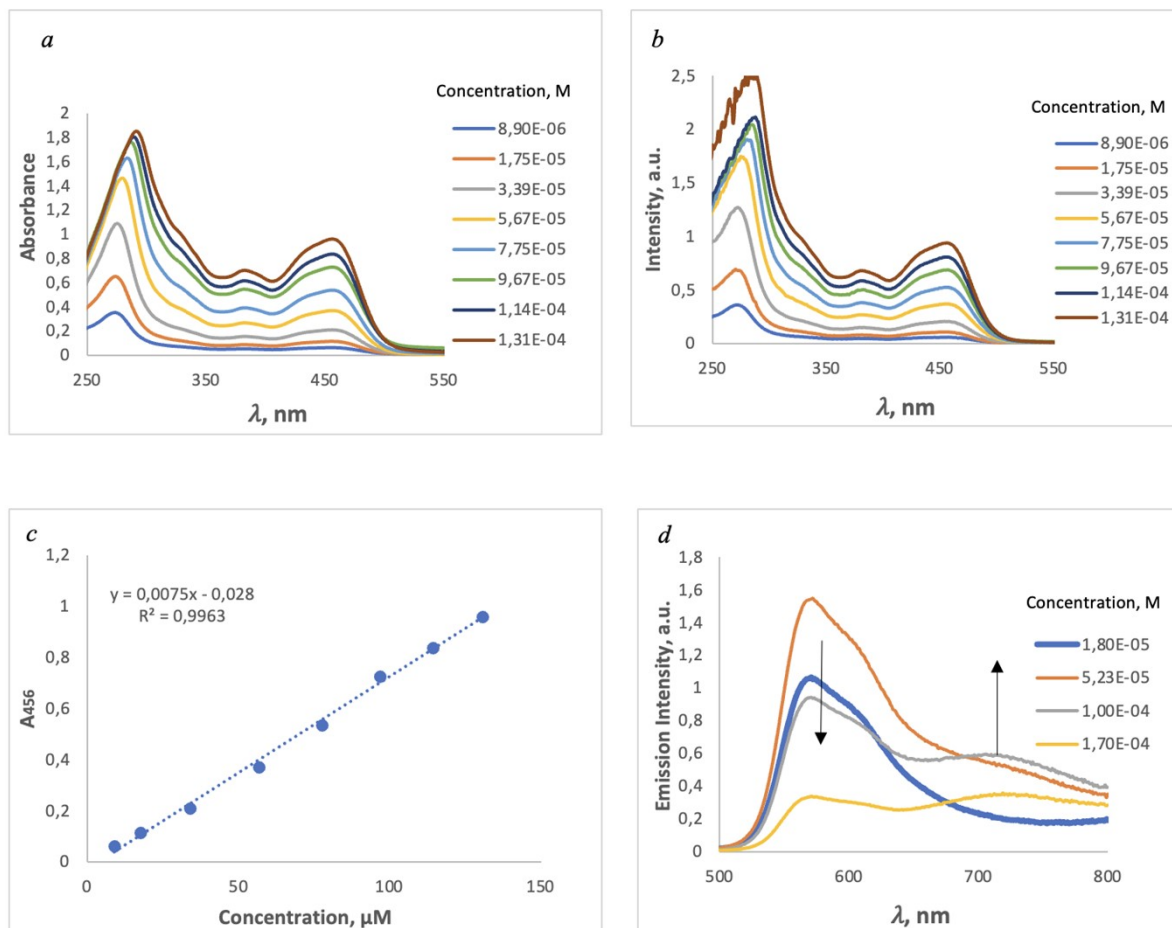


Fig. S28 Photophysical Data for Complex 2 *a)* Absorption spectra at different concentration in CH_2Cl_2 solution; *b)* excitation spectra at different concentration in CH_2Cl_2 solution; *c)* Beer-Lambert law ; *b)* emission spectra at different concentration in deoxygenated CH_2Cl_2 solution, $\lambda_{\text{exc}} = \lambda_{\text{max}}^{\text{abs}}$ of the lowest energy band.

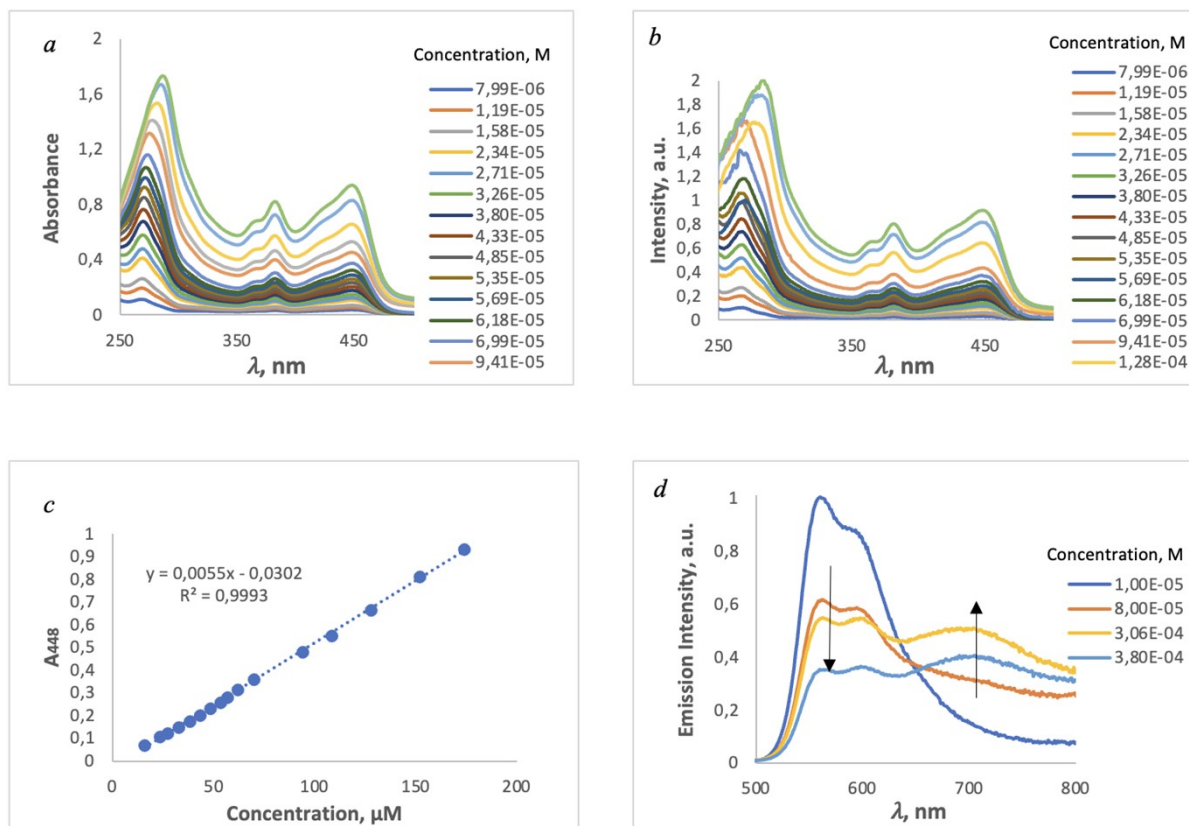


Fig. S29 Photophysical Data for Complex 8 *a)* Absorption spectra at different concentration in CH_2Cl_2 solution; *b)* excitation spectra at different concentration in CH_2Cl_2 solution; *c)* Beer-Lambert law; *d)* emission spectra at different concentration in deoxygenated CH_2Cl_2 solution, $\lambda_{\text{exc}} = \lambda_{\text{max}}^{\text{abs}}$ of the lowest energy band.

Additional Theoretical Results

Table S4. Major computed optical transitions λ (nm) contributing to the simulated absorption band of lowest energy (see Table 3) and their dominant character. Oscillator strengths are provided in parentheses.

| | λ (osc. strenght) | Major contribution |
|-----------|---------------------------|----------------------------|
| 1 | 386 (0.1293) | H->L (+96%) |
| 2 | 429 (0.1313) | H->L (+91%) |
| 3 | 383 (0.1117) | H->L (+96%) |
| 4 | 422 (0.0156) | H->L (+98%) |
| | 386 (0.0566) | H-1→L+1 (79%), H→L+1 (19%) |
| 5 | 464 (0.1475) | H->L (+97%) |
| 6 | 420 (0.2341) | H→L (97%) |
| | 395 (0.0619) | H->L (96%) |
| | 384 (0.1139) | H-1→L+1 (95%) |
| 7 | 461 (0.1037) | H→L (83%), H→L+1 (15%) |
| | 448 (0.1006) | H→L+1 (82%), H→L (15%) |
| 8 | 482 (0.1274) | H→L+1 (62%), H→L (35%) |
| | 470 (0.0746) | H→L (61%), H→L+1 (35%) |
| 9 | 433 (0.0485) | H→L (67%), H→L+1 (31%) |
| | 424 (0.1354) | H→L+1 (67%), H→L (31%) |
| 10 | 434 (0.0614) | H→L (75%), H→L+1 (23%) |
| | 425 (0.1338) | H→L+1 (74%), H→L (23%) |
| 11 | 505 (0.2127) | H→L (71%), H→L+1 (20%) |
| | 490 (0.0434) | H→L+1 (72%), H→L (20%) |
| 12 | 434 (0.1577) | H→L+1 (97%) |
| 13 | 467 (0.1745) | H→L+1 (97%) |
| 14 | 385 (0.0851) | H-1→L+1 (97%) |
| | 384 (0.0928) | H-1→L (95%) |

Table S5. Relevant computed interatomic distances (in Å) and corresponding Wiberg bond indices (WBI) into bracket. for complexes **1-14**.

| Compound | 1 | 2 | 3 | 4 | 5 | 6 | 7 | 8 | 9 | 10 | 11 | 12 | 13 | 14 |
|--------------------------------------|------------------|------------------|------------------|------------------|------------------|------------------|------------------|------------------|------------------|------------------|------------------|------------------|------------------|------------------|
| Pt-N [WBI] | 2.035 [0.414] | 2.035 [0.414] | 2.036 [0.414] | 2.038 [0.414] | 2.038 [0.414] | 2.039 [0.413] | 2.039 [0.414] | 2.039 [0.414] | 2.040 [0.412] | 2.041 [0.412] | 2.040 [0.414] | 2.038 [0.414] | 2.038 [0.414] | 2.040 [0.413] |
| Pt-C_{NACAN} [WBI] | 1.905 [0.776] | 1.906 [0.763] | 1.901 [0.784] | 1.939 [0.630] | 1.938 [0.631] | 1.940 [0.628] | 1.940 [0.620] | 1.939 [0.621] | 1.941 [0.619] | 1.941 [0.619] | 1.940 [0.621] | 1.935 [0.636] | 1.935 [0.638] | 1.937 [0.635] |
| Pt-Cl or Pt-CCR [WBI] | 2.425 [0.288] | 2.424 [0.289] | 2.421 [0.294] | 2.047 [0.474] | 2.047 [0.474] | 2.043 [0.480] | 2.046 [0.477] | 2.047 [0.476] | 2.042 [0.482] | 2.042 [0.482] | 2.047 [0.477] | 2.045 [0.478] | 2.045 [0.477] | 2.042 [0.482] |
| C≡C [WBI] | - | - | - | 1.225 [2.741] | 1.225 [2.742] | 1.226 [2.709] | 1.225 [2.736] | 1.226 [2.740] | 1.226 [2.707] | 1.226 [2.704] | 1.226 [2.732] | 1.225 [2.740] | 1.225 [2.742] | 1.225 [2.713] |

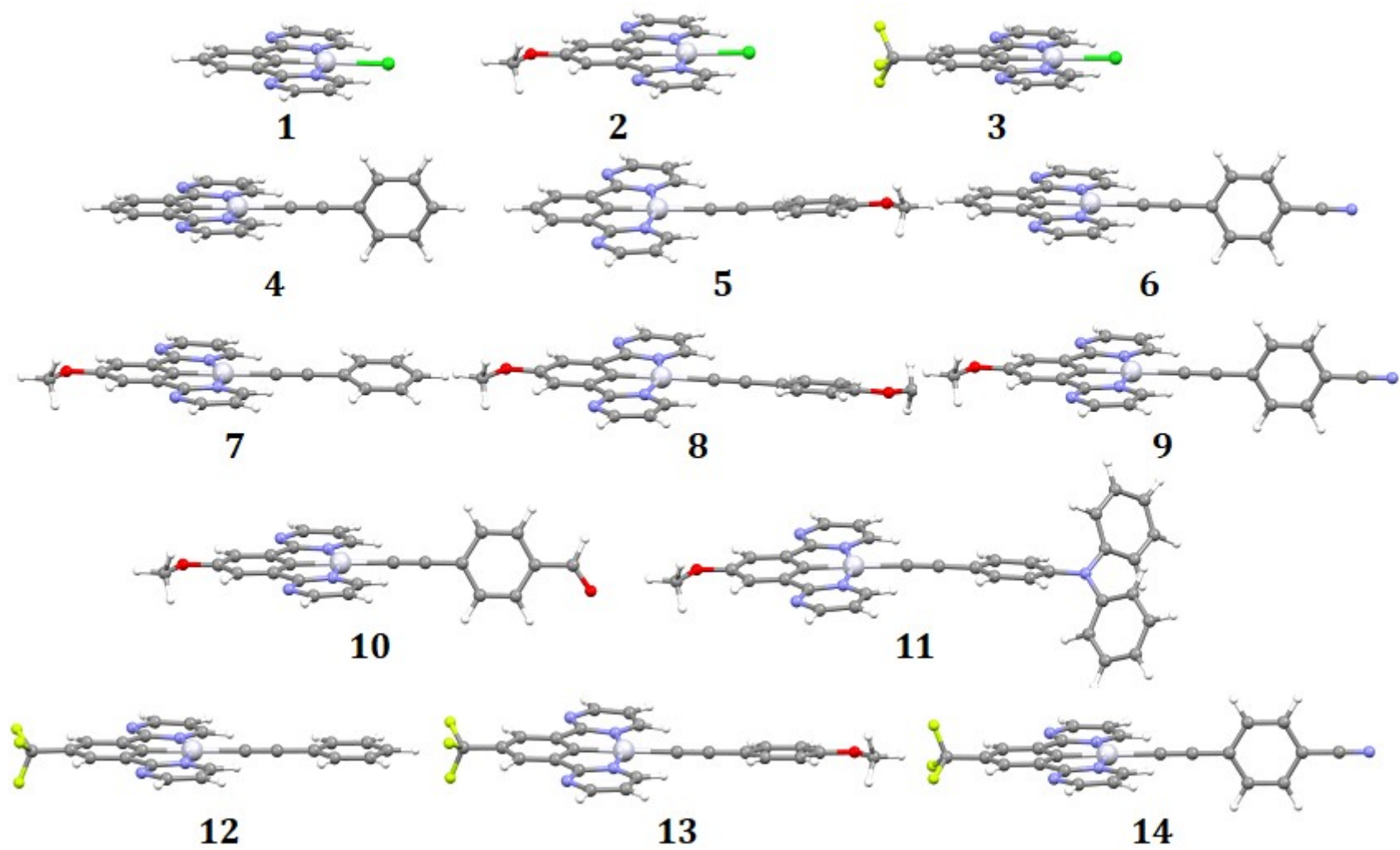


Fig. S30 DFT-optimized structures of compounds 1-14.

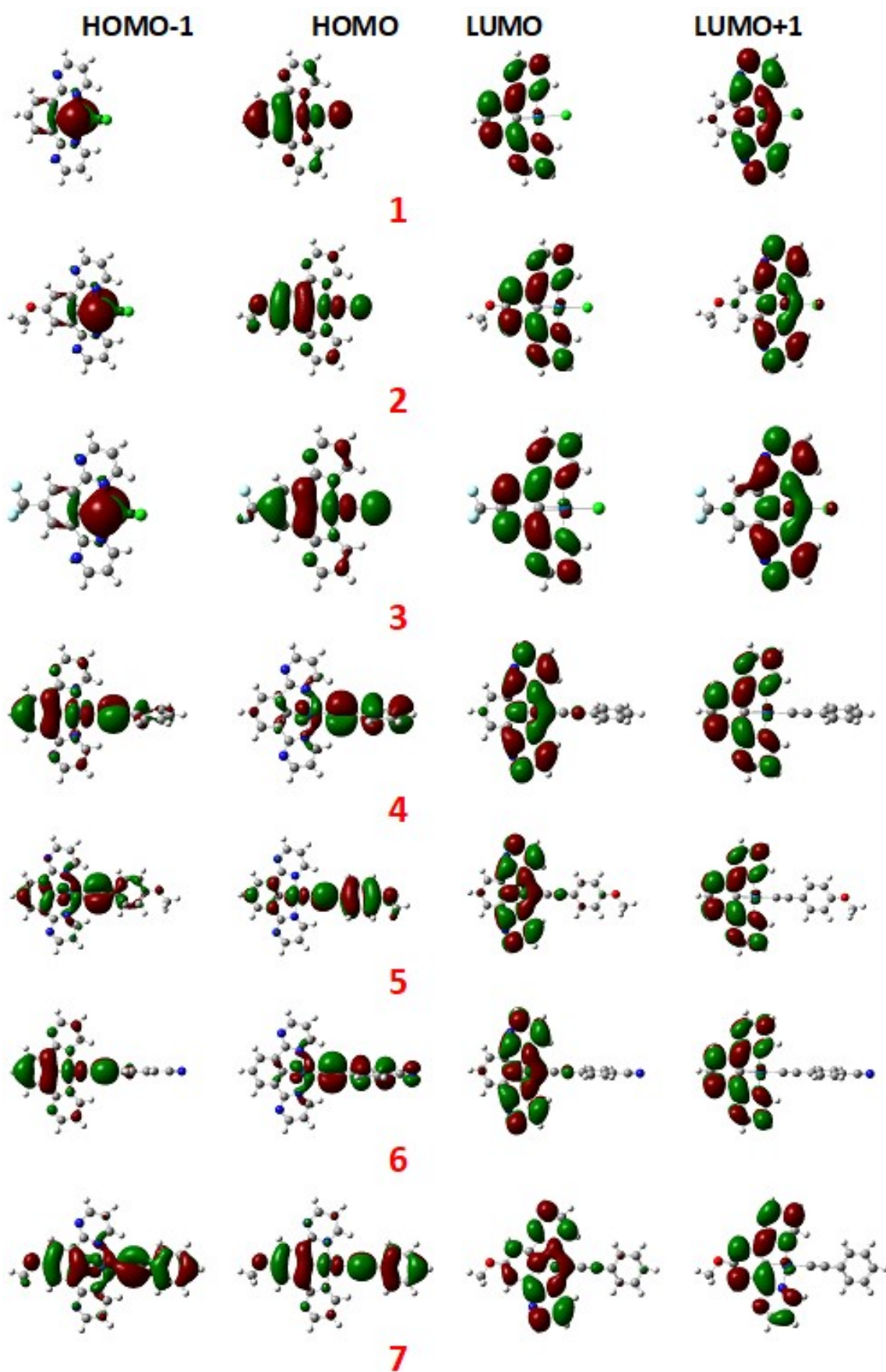


Fig. S31a The frontier orbitals of complexes 1-7

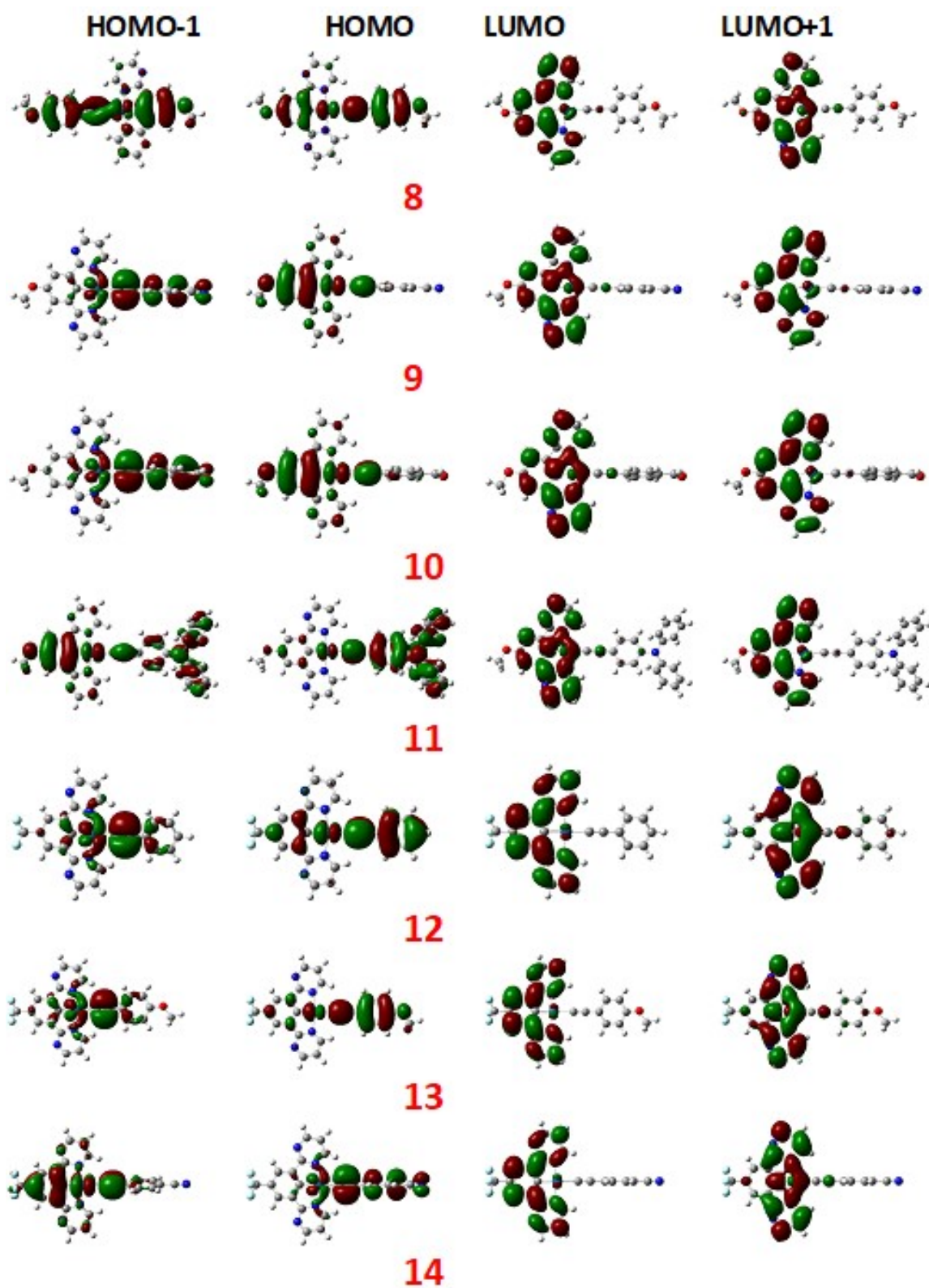


Fig. S31b The frontier orbitals of complexes 8-14

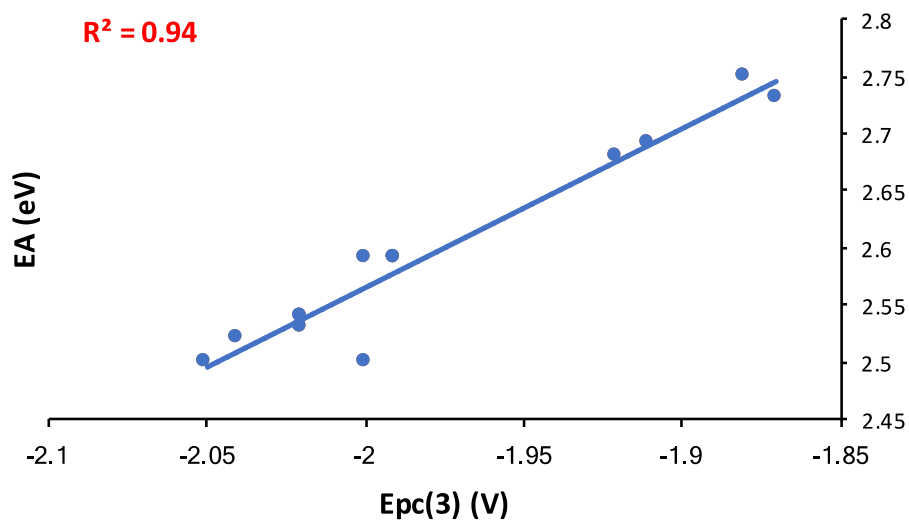


Fig. S32 Relationship between the experimental electrochemical $E_{pc}(3)$ values and the DFT-computed electron affinities (EA).

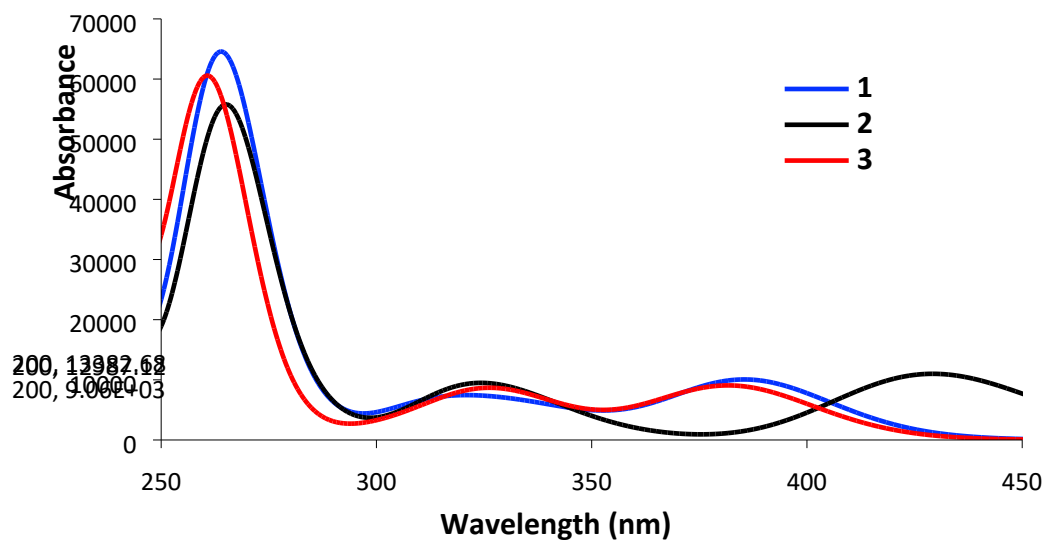


Fig. S33 TD-DFT-simulated UV/vis spectra of compounds **1-3**

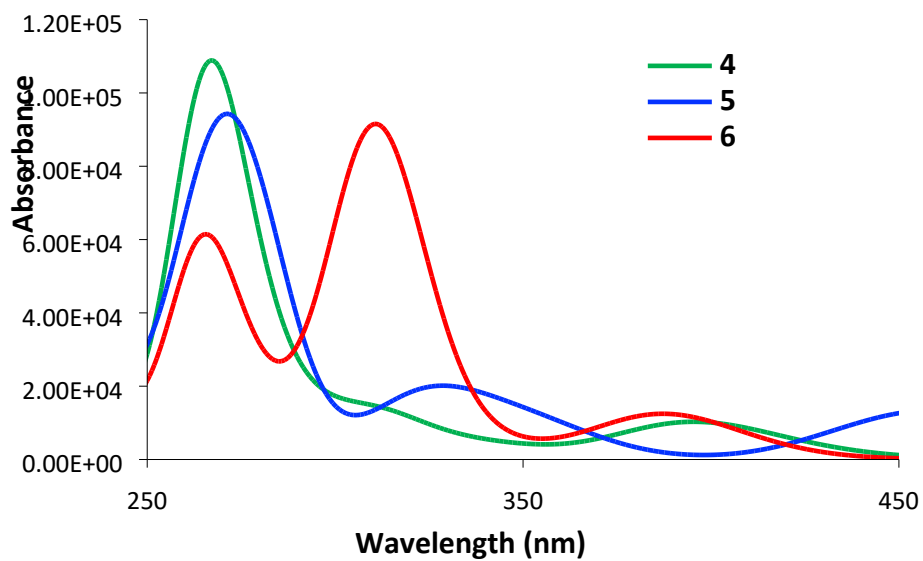


Fig. S34 TD-DFT-simulated UV/vis spectra of compounds 4-6

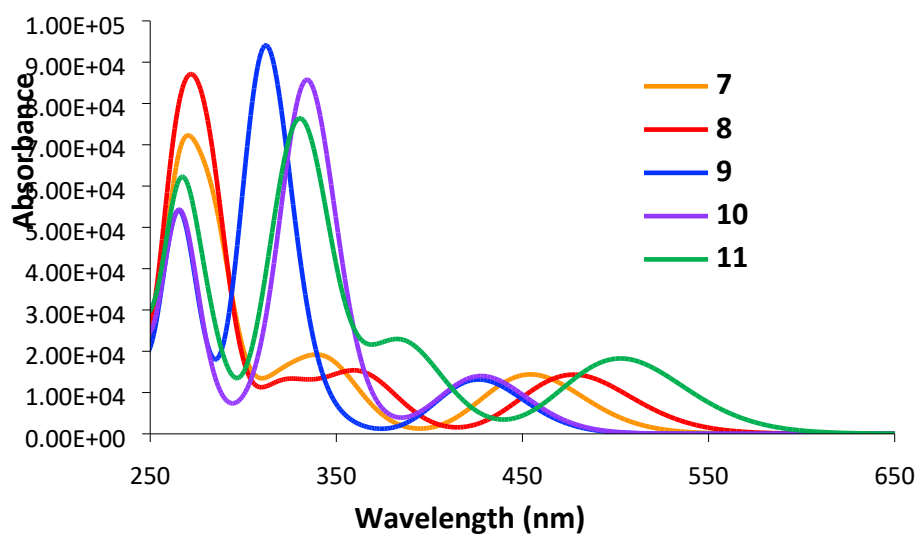


Fig. S35 TD-DFT-simulated UV/vis spectra of compounds 7-11

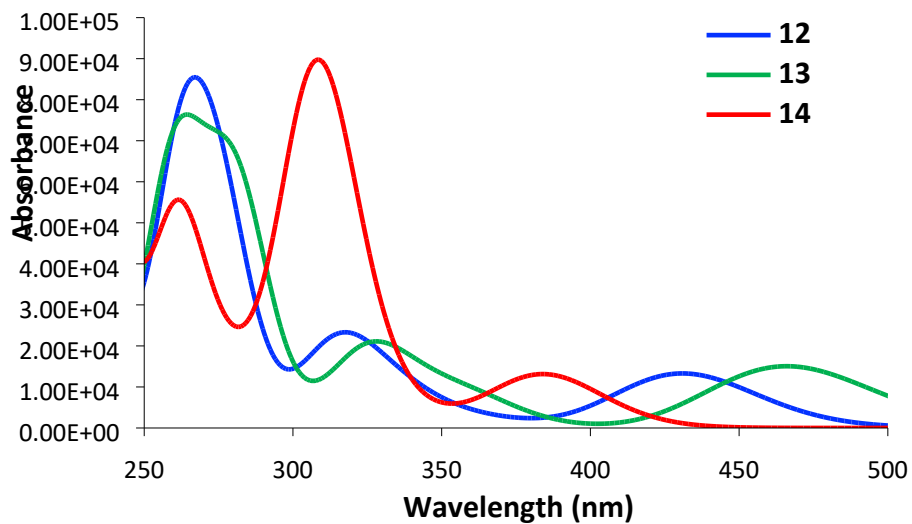


Fig. S36 TD-DFT-simulated UV/vis spectra of compounds **12-14**

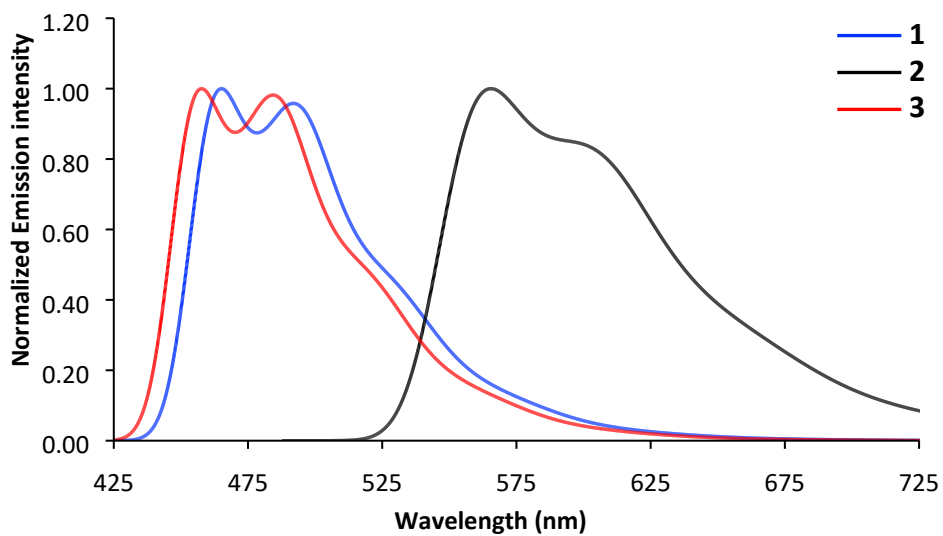


Fig. 37 DFT-simulated phosphorescence spectra of compounds **1-3**

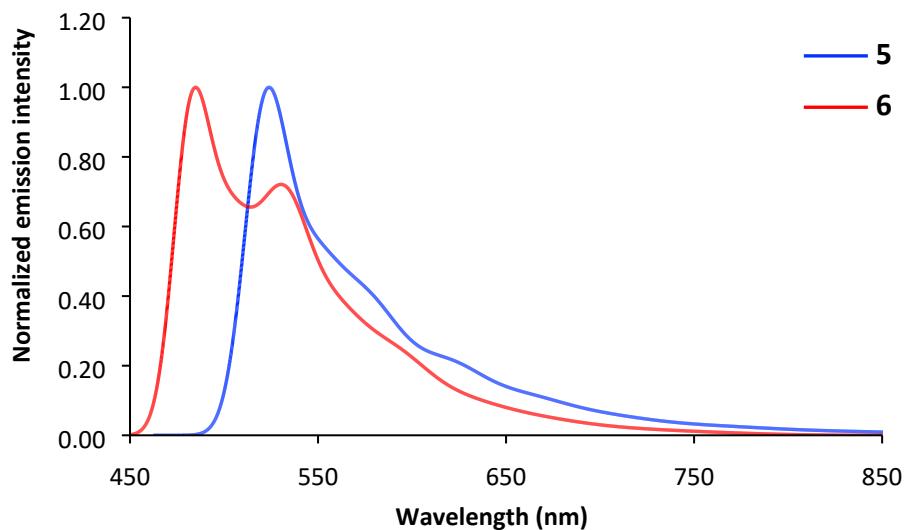


Fig. S38 DFT-simulated phosphorescence spectra of compounds **5** and **6**

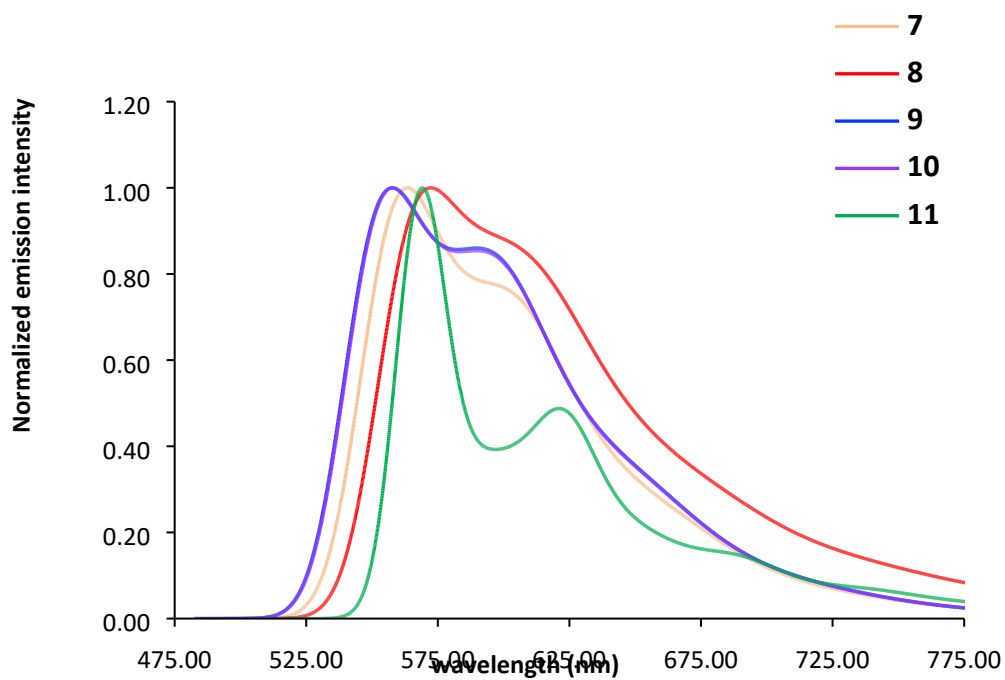


Fig. S39 DFT-simulated phosphorescence spectra of compounds **7-11**

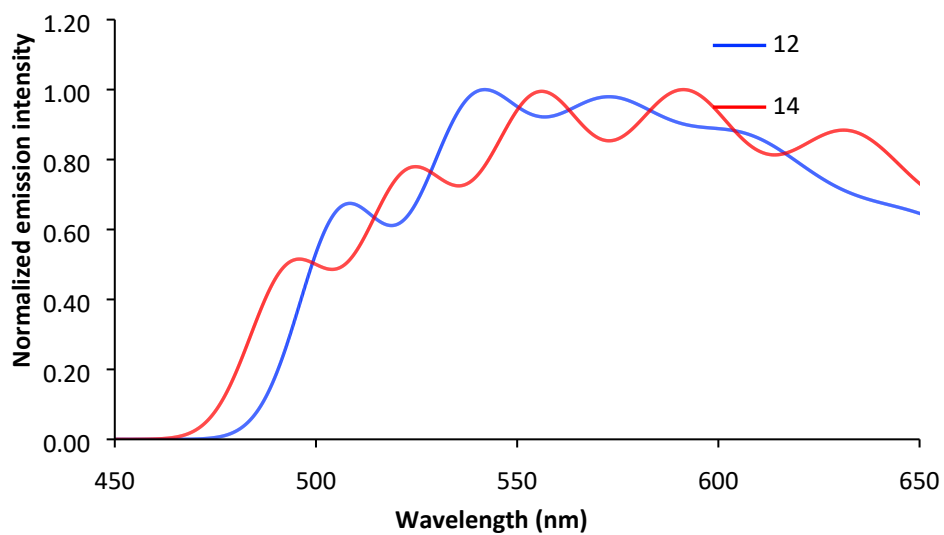


Fig. S40 DFT-simulated phosphorescence spectra of compounds **12** and **14**

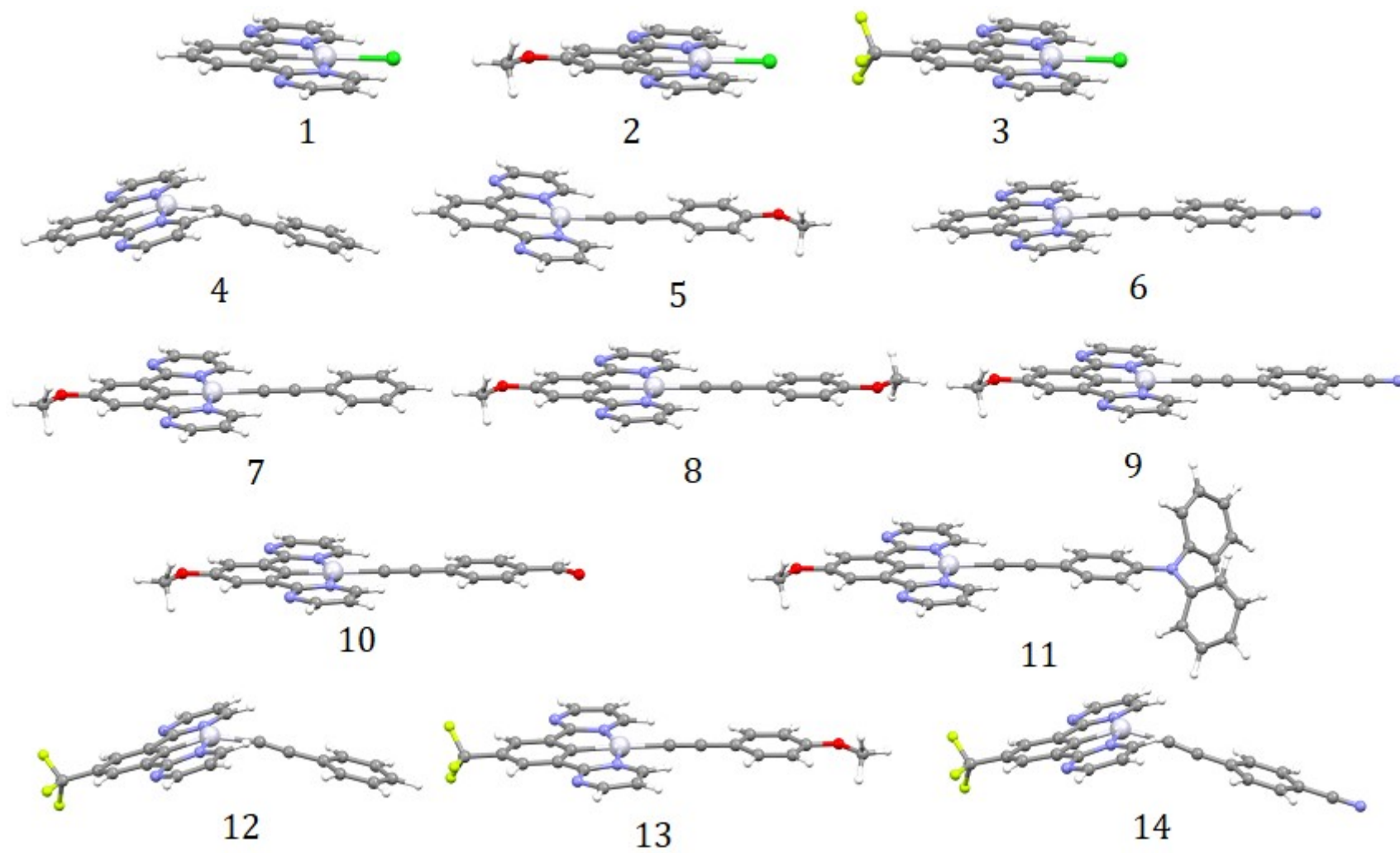


Fig. S41 DFT-optimized structures of the lowest triplet stated of compounds **1-14**.

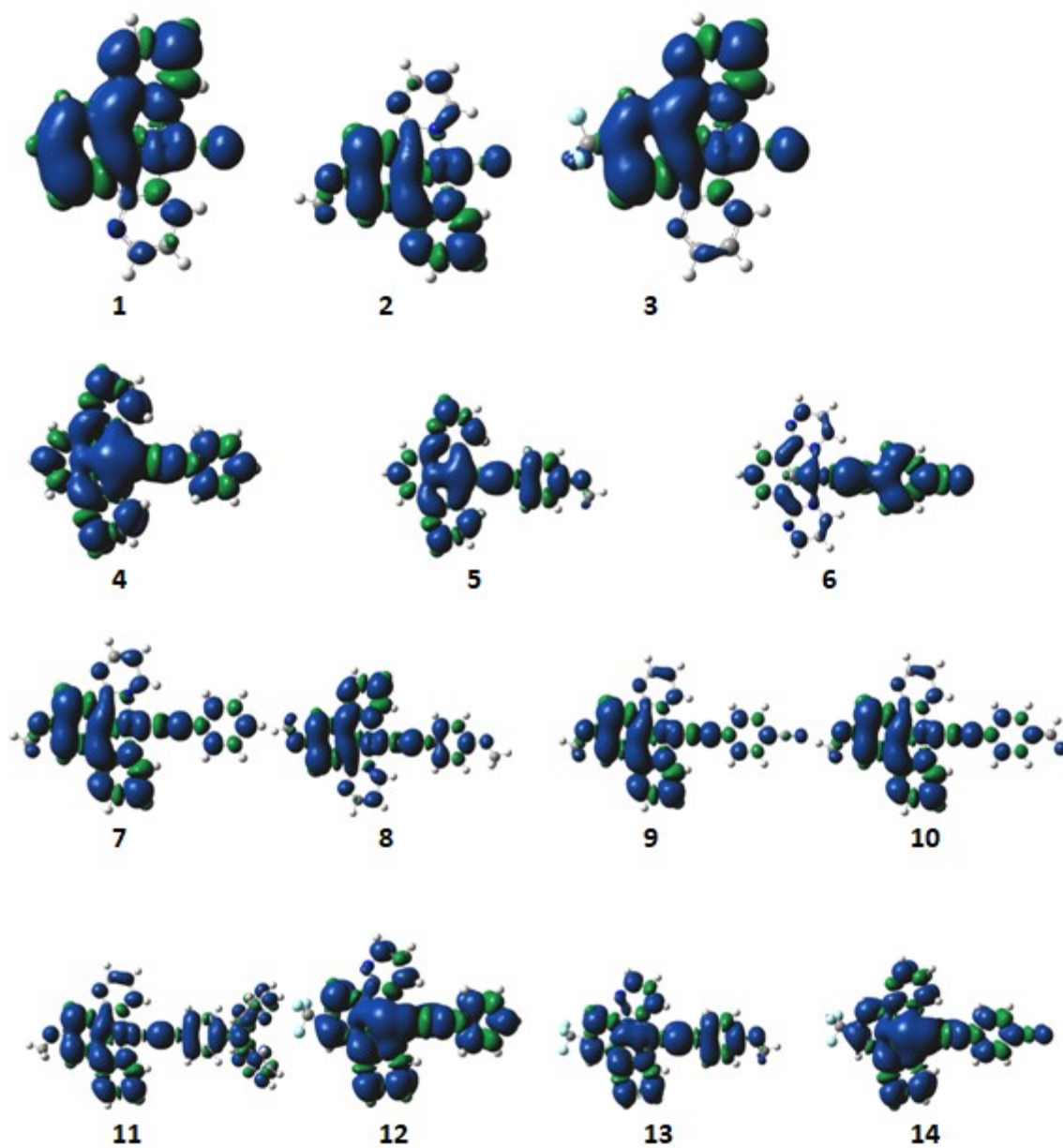


Fig. S42 Spin densities of the lowest triplet state of complexes **1-14**.

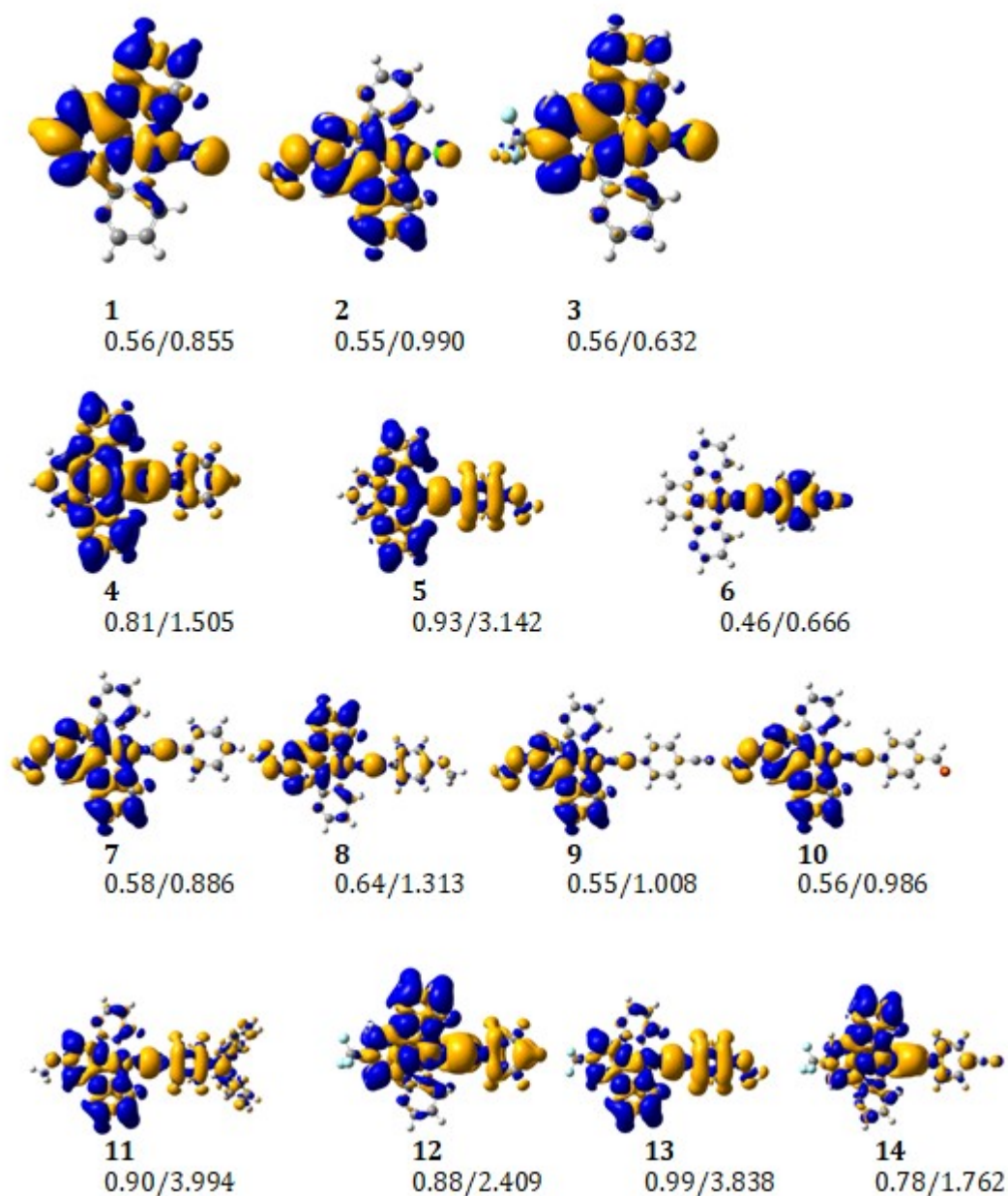


Fig. S43 Density difference plots associated with the triplet→singlet emissive transitions. The blue and yellow colors indicate an increase and decrease of density upon de-excitation, respectively. The numerical values are the computed charge transfers (q^{CT}) and corresponding distance transfer (d^{CT} , in Å), respectively (see Computational details).

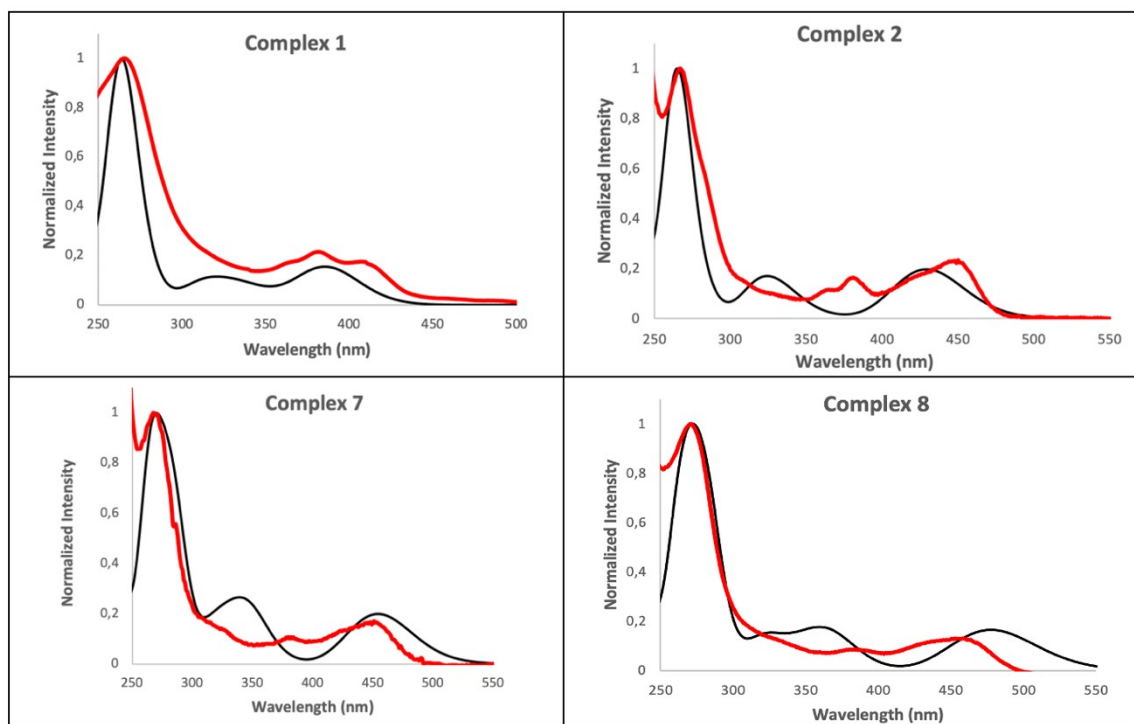


Fig. S44 Comparison of absorption spectra theoretical (black line) and practical (red line) of complexes **1**, **2**, **7** and **8** in CH_2Cl_2 solution

References

- [1] Sheldrick, G. M. SHELXT - Integrated Space-group and Crystal-structure Determination. *Acta Cryst.*, **2015**, A71, 3–8.
- [2] Sheldrick, G. M. Crystal Structure Refinement with SHELXL. *Acta Cryst.*, **2015**, C71, 3–8.